

Acquired FGFR and FGF alterations confer resistance to estrogen receptor (ER) targeted therapy in ER+ metastatic breast cancer

Pingping Mao^{1,2,3,4,£}, Ofir Cohen^{1,2,3,4,£}, Kailey J. Kowalski^{1,2,3,4}, Justin G. Kusiel^{1,2,3,4}, Jorge E. Buendia-Buendia^{1,2,3,4}, Michael S. Cuoco⁷, Pedro Exman², Seth A. Wander^{1,2,3,4,5}, Adrienne G. Waks^{1,2,3,4,5}, Utthara Nayar^{1,2,3,4}, Jon Chung⁶, Samuel Freeman⁴, Orit Rozenblatt-Rosen⁷, Vincent A. Miller⁶, Federica Piccioni⁴, David E. Root⁴, Aviv Regev^{7,8}, Eric P. Winer^{2,3,5}, Nancy U. Lin^{2,3,5}, Nikhil Wagle^{1,2,3,4,5}

1. Center for Cancer Precision Medicine, Dana-Farber Cancer Institute, Boston, MA
2. Department of Medical Oncology, Dana-Farber Cancer Institute, Boston, MA
3. Harvard Medical School, Boston, MA
4. Broad Institute of MIT and Harvard, Cambridge, MA
5. Department of Medicine, Brigham and Women's Hospital, Boston, MA
6. Foundation Medicine, Inc. Cambridge, MA
7. Klarman Cell Observatory, Broad Institute of MIT and Harvard, Cambridge MA
8. Howard Hughes Medical Institute and Koch Institute of Integrative Cancer Research, Department of Biology, Massachusetts Institute of Technology, Cambridge, MA

Running title: FGFR/FGF alterations confer resistance to endocrine therapy

Key words: Drug resistance, endocrine therapy, ER+ breast cancer, FGF, FGFR

*Address correspondence to:

Nikhil Wagle, MD
Department of Medical Oncology
Dana-Farber Cancer Institute
450 Brookline Ave, Dana 820A
Boston, MA 02215
Phone: 617-632-6419
e-mail: nikhil_wagle@dfci.harvard.edu

£These authors contributed equally

Word count (excluding abstract, methods, references and figure legends): 5280

Total number of figures: 6

Competing Financial Interest Statement

S.A.W. is a consultant for Foundation Medicine and Eli Lilly, and a consultant and equity holder for InfiniteMD. J.C. is an employee/stockholder in Foundation Medicine, a wholly owned subsidiary of Roche. V.A.M. is an employee of Foundation Medicine/Roche, officer and board member of Revolution Medicines, and stockholder of Roche and Revolution Medicines. N.U.L is a consultant for Puma Biotechnology and Daichii, and received research funding from Pfizer, Genentech, Novartis and Seattle Genetics. A.R. is

a SAB member of ThermoFisher Scientific, Syros Pharmaceuticals, and Neogene Therapeutics, and a founder of and equity holder in Celsius Therapeutics. E.P.W. is a consultant for InfiniteMD, Genentech, and Eli Lilly. N.W. was previously a stockholder and consultant for Foundation Medicine; has been a consultant/advisor for Novartis and Eli Lilly; and has received sponsored research support from Novartis and Puma Biotechnology. None of these entities had any role in the conceptualization, design, data collection, analysis, decision to publish, or preparation of the manuscript.

Translational Relevance

A genome-scale overexpression screen revealed a broad spectrum of resistance mechanisms against SERDs, which can provide a resource for researchers studying resistance to ER-directed therapies as well as the biology of estrogen receptor dependencies in ER+ breast cancer. We demonstrate that activating FGFR/FGF alterations are a mechanism of acquired resistance to ER-directed therapies and CDK4/6 inhibitors in ER+ metastatic breast cancer and can be overcome by combination therapy targeting both the ER and the FGFR pathway. The detection of targetable, clonally acquired genetic alterations in metastatic tumor biopsies highlights the value of serial tumor testing to dissect mechanisms of resistance in human breast cancer and its potential application in directing clinical management.

Abstract

Purpose: To identify clinically relevant mechanisms of resistance to ER-directed therapies in ER+ breast cancer.

Experimental design: We conducted a genome-scale functional screen spanning 10,135 genes to investigate genes whose overexpression confer resistance to selective estrogen receptor degraders. In parallel, we performed whole exome sequencing in paired pre-treatment and post-resistance biopsies from 60 patients with ER+ metastatic breast cancer who had developed resistance to ER-targeted therapy. Furthermore, we performed experiments to validate resistance genes/pathways and to identify drug combinations to overcome resistance.

Results: Pathway analysis of candidate resistance genes demonstrated that the FGFR, ERBB, insulin receptor, and MAPK pathways represented key modalities of resistance. The FGFR pathway was altered via *FGFR1*, *FGFR2*, or *FGF3* amplifications or *FGFR2* mutations in 24 (40%) of the post-resistance biopsies. In 12 of the 24 post-resistance tumors exhibiting FGFR/FGF alterations, these alterations were acquired or enriched under the selective pressure of ER-directed therapy. *In vitro* experiments in ER+ breast cancer cells confirmed that FGFR/FGF alterations led to fulvestrant resistance as well as cross-resistance to the CDK4/6 inhibitor palbociclib. RNA sequencing of resistant cell lines demonstrated that FGFR/FGF induced resistance through ER reprogramming and activation of the MAPK pathway. The resistance phenotypes were reversed by FGFR inhibitors, a MEK inhibitor, and/or a SHP2 inhibitor.

Conclusions: Our results suggest that FGFR pathway is a distinct mechanism of acquired resistance to ER-directed therapy that can be overcome by FGFR and/or MAPK pathway inhibitors.

Introduction

Approximately 70% of breast cancers express the estrogen receptor (ER), and estrogen signaling drives breast cancer cell growth and progression [1]. Although endocrine therapies, including tamoxifen, aromatase inhibitors (AI), and the selective estrogen receptor degrader (SERD) fulvestrant have improved survival for ER+ breast cancer patients, within the metastatic setting resistance to endocrine therapies is nearly universal [2].

Although various resistance mechanisms have been proposed for tamoxifen and aromatase inhibitor resistance, including loss or modification in ER expression (*ESR1* activating mutations and *ESR1* fusions) [3-7], and regulation of alternative signal transduction pathways (PI3K/AKT/mTOR and EGFR/ERBB2/MAPK) [8-10], mechanisms of resistance to SERDs remain understudied. Mechanisms of endocrine resistance identified in patients include acquired mutations in the estrogen receptor itself [4-7], acquired activating mutations in *ERBB2* (HER2) [11, 12], loss of function of *NFI* [13], and other alterations in MAPK pathway genes [14]. Additional clinically relevant mechanisms remain to be identified.

Gain-of-function screens have played a pivotal role in identification of resistance mechanisms to targeted therapies in various cancer types [15-17]. In breast cancer, several functional screen studies identified *IGF1R*, *KRAS* and *ESR1* as mechanisms of resistance to tamoxifen and/or estrogen deprivation [18-20]. However, genome-scale functional screens for SERD resistance have not been reported.

We conducted a genome-scale gain-of-function screen in ER+ breast cancer cells spanning 17,255 overexpressed lentiviral open reading frames (ORFs) to investigate genes whose overexpression was sufficient to confer resistance to the SERDs fulvestrant and GDC-0810 [21]. In parallel, we sought to identify endocrine resistance mechanisms of clinical significance through genomic profiling of paired pre-treatment and post-treatment tumor samples from 60 patients with ER+ metastatic breast cancer (MBC) who developed resistance to endocrine therapy.

Methods

Cell culture

293T, T47D and MCF7 cells were obtained directly from American Type Culture Collection (ATCC) as frozen vials and were cultured as described in the Supplemental Methods. MCF7 and T47D were validated by western blotting for ER and HER2 (based on known genotype). We used cell lines of passage number ranging from 4 to 15 in the described experiments. All cell lines tested negative for mycoplasma contamination by ATCC Universal Mycoplasma Detection Kit. The last test was performed in November 2019.

Genome-scale gain-of-function screen

The pooled lentiviral ORF library hORFeome [22] consists of 17,255 barcoded human open reading frames (ORFs), corresponding to 10,135 distinct human genes with at least 99% nucleotide and protein match. These ORFs were cloned into pLX317 vector and

pooled together for transfection into 293T cells to make pooled lentivirus (with 2nd generation packaging plasmids). In 6-well plates, pooled lentivirus was infected in cells to achieve ~50% infection rate and ensure ~1000 infected cells per ORF for 17255 ORFs. Media was supplemented with 4 µg/mL polybrene (Thermo Fisher Scientific # TR1003G) to boost transfection efficiency. After infection, cells were pooled and selected with 1.5 µg/mL puromycin for 5 days. Upon completion of selection, cells were plated for three different drug conditions: DMSO, 100 nM fulvestrant, 1 µM GDC-0810. There were three replicates for each condition screened. A subset of cells was saved for sequencing as early time point (ETP) samples to confirm ORF representation. Infected cells were passaged upon confluency and maintained in DMSO or drugs for 21 days to allow sufficient time for cells carrying resistance to be enriched from the population. At the end of the time course, cells were harvested for isolating genomic DNA as late time point samples (LTP). All genomic DNA samples were amplified with PCR primers flanking the ORF region and sequenced. The ORF representation at the final harvesting (LTP) is compared to the representation of ORFs in cells collected before drug addition (ETP). Cells carrying ORFs that are driving resistance will grow and gradually enrich the population and therefore, will be over-represented in the sequencing data for the final passage compared to the early time point. An ORF with significant enrichment (a Z score >3) is defined as a resistance candidate gene. A secondary validation screen was performed as described in the Supplemental Methods.

Patients and tumor samples

Prior to any study procedures, all patients provided written informed consent for research biopsies and whole exome sequencing of tumor and normal DNA, as approved by the Dana-Farber/Harvard Cancer Center Institutional Review Board (DF/HCC Protocol 05-246). Metastatic core biopsies were obtained from patients and samples were immediately snap frozen in OCT and stored in -80°C. Archival FFPE blocks of primary tumor samples were also obtained. A blood sample was obtained during the course of treatment, and whole blood was stored at -80°C until DNA extraction from peripheral blood mononuclear cells (for germline DNA) was performed. In a few instances, cell free DNA was obtained from plasma for circulating tumor DNA analysis, as previously described[23]. The studies were conducted in accordance with U.S. Common Rule for ethical guidelines.

Whole Exome Sequencing (WES) analysis

DNA was extracted from primary tumors, metastatic tumors, plasma, and peripheral blood mononuclear cells (for germline DNA) from all patients and whole exome sequencing was performed, as detailed in the Supplemental Methods. Sequencing data were analyzed using tools to identify somatic point mutations and small insertions/deletions (indels), and copy number changes using established algorithms (see Supplemental Methods).

To better measure segment-specific copy-number, we subtracted the genome ploidy for each sample to compute copy number above ploidy (CNAP). CNAP of at least 3 are considered as amplifications (AMP), CNAP below 3 are considered low amplification

and ignored in our analysis). CNAP of at least 6 are considered high amplifications (HighAMP), and CNAP of at least 9 and fewer than 100 genes [24] is considered very high focal amplification (FocalAMP).

The evolutionary classification of amplifications accounts for the magnitude of the observed copy-number difference between the pre-treatment and the post-treatment samples. We used the same method as previously described to make the evolutionary classifications [25]. If the difference between the CNAP of the post-treatment and the CNAP of the pre-treatment is smaller than 50%, the amplification is defined as “Shared”. If the CNAP of the post-treatment is larger than the CNAP by more than 50% and the lower pre-treatment CNAP is not at “FocalAMP” level, the evolutionary classification is “Acquired”. If CNAP of the post-treatment is smaller by at least 50%, comparing to the pre-treatment sample and the lower post-treatment CNAP is not at “FocalAMP” level, the evolutionary classification is “Loss”. Otherwise, the evolutionary classification of amplifications is defined as “Indeterminate”.

RNA-seq characterization of genomically perturbed cells under various drug conditions

We performed RNA-Seq on T47D cells perturbed to overexpress FGFR pathway activation including FGFR1, FGFR2 (WT, K660N, M538I and N550K), and FGF3, as well as GFP and parental as a control, as described above. Cells were plated in 96-well plates, and then treated with DMSO, fulvestrant (100 nM), palbociclib (1 μ M), FIIN-3 (100 nM), and trametinib (500 nM) as single agent and in combinations for 24 hours.

FGFR1/2 cell lines were treated with or without FGF2 (10 ng/mL) in various conditions. RNA was extracted from cells and sequencing libraries prepared as described in Supplementary Methods. For each specific construct and treatment combination we performed at least 6 replicates, for a total of 672 RNA-Seq profiles.

Generation of plasmids and engineered cells

T47D or MCF7 cells were infected with lentivirus to derive stable cell lines overexpressing wildtype (WT) or mutant ORFs. All WT ORFs were obtained from the Broad Institute. Mutant ORFs (FGFR2 M538I, N550K and K660N) were made using QuickChange II site-directed mutagenesis kit (Agilent Technologies #200523). Most stable cells lines express ORFs in pLX317 vector and were selected with puromycin (Life Technologies #A1113803). Stable cell lines expressing CCND1 and PIM1 in pLX304 vector were selected with blasticidin (Life Technologies #A1113903).

Kill curves and CellTiter-Glo viability assay

Cells were plated in 96-well tissue culture ViewPlate (Perkin Elmer # 6005181) on Day 1 and treated with drug on Day 2. Media with or without drugs was refreshed on Day 5. On Day 8, cells were equilibrated to room temperature, media was removed, and cells were lysed in a mixture of 50 μ L media and 50 μ L CellTiter-Glo 2.0 reagent (Promega # G9243) per well. Plates were then incubated on an orbital shaker for 2 mins. Following another 10 mins of incubation at room temperature to stabilize signal, luminescence was recorded to measure cell viability on Infinite M200 Pro microplate reader (Tecan).

Western blotting

Western blotting was performed as described in supplemental methods.

Statistical analysis

Statistical analyses related to drug response curve were performed with two-tailed student t-test in Graphpad Prism. Fisher's exact test was used to calculate odds ratio and q-value for volcano plots in the RNA sequencing analysis. Cohen's D test with Hedges correction and Welch's t-test were used to estimate the effect size and significance for signature strength of gene sets.

Results

A genome-scale gain-of-function screen for resistance to selective estrogen receptor degraders

To identify the spectrum of genes whose overexpression confers resistance to SERDs *in vitro*, we expressed a pooled lentiviral library of 17,255 human open reading frames (ORFs), corresponding to 10,135 distinct human genes, in ER+ T47D breast cancer cells in the presence of fulvestrant or GDC-0810 [22]. Genes that confer drug resistance will be enriched under drug selection for 21 days, indicated by a positive log fold change (LFC) for ORF representation before and after DMSO/drug selection.

Using a Z score >3 as a criterion to identify resistance candidates, we identified 64 genes (93 ORFs) that conferred resistance to fulvestrant and 57 genes (83 ORFs) that conferred resistance to GDC-0810 (Fig.1A and Supplemental Table.1). 37 genes (55 ORFs)

conferred resistance to both drugs, a degree of overlap which was anticipated given the mechanistic similarities between fulvestrant and GDC-0810. The LFC and corresponding Z score for each ORF in fulvestrant and GDC-0810 treatment arms were highly correlated, with a correlation coefficient of 0.77 (Fig.1A).

To confirm these results, we conducted a secondary screen using a smaller pooled library consisting of 570 ORFs in T47D and MCF7 cells to validate candidates nominated by the primary screen. Both cell lines are commonly used and well-characterized ER+ breast cancer cell and both are sensitive to SERDs, though they have different levels of ER signaling and harbor some genomic differences (<https://portals.broadinstitute.org/ccle>) [26, 27]. Top resistance genes found in the primary screen were again enriched in the secondary screen for T47D cells, including *FGF* genes, *FOXRI*, *AKT* genes, *PIM* genes and several *GPCR* genes (Supplemental Data Fig.S1A). Many top ranked resistance genes (*CSF1R*, *FGF3*, *FGF6*, *FOXRI* and *PIM2*) were shared between T47D and MCF7 cells (Supplemental Data Fig.S1B). However, distinct resistance genes were also observed in each cell line, suggesting some resistance mechanisms may be cell context-dependent.

Functional categories of candidate resistance genes include serine/threonine kinases (*PIK3CA*, *AKT1/2/3*, *PIM1/2/3*), receptor tyrosine kinases (*EGFR*, *ERBB2*, *PDGFRB*), growth factors (*FGF3/6/10/22*), cell cycle regulatory proteins (*CCND1*, *CCND2*, *CCND3*, *CDK6*) and G-protein coupled receptors (*GPCR*) (Fig.1B). As further validation, we overexpressed 13 ORFs belonging to these categories individually in

T47D cells and they conferred resistance to fulvestrant and GDC-0810 to various degrees (Fig.1C and Supplemental Data Fig.S2A-B).

Gene Set Enrichment Analysis (GSEA) of the candidate resistance genes demonstrated enrichment in 4 functional pathways: FGFR signaling, ERBB signaling, insulin receptor signaling, and the MAPK pathway (Fig.1D, Supplemental Data Fig.S3 and Supplemental Table.2). Consistent with this, we and others recently demonstrated that *ERBB2* activating mutations [11] and alterations in MAPK pathway genes can cause endocrine resistance in patients with ER+ MBC [13, 14, 25]. We sought to further examine the role of FGFR and FGF genes in resistance to SERDs in MBC.

Identification of acquired FGFR and FGF alterations in metastatic biopsies from patients with resistant ER+ MBC

To examine the potential role of FGFR and FGF alterations in the development of endocrine resistance clinically, we analyzed whole exome sequencing (WES) data from paired pre-treatment and post-treatment metastatic tumor biopsies or cell free DNA from 60 patients with ER+ metastatic breast cancer who had received at least one endocrine therapy (tamoxifen, AI, SERDs) for more than 120 days between the two biopsies [28].

Amongst the 60 post-treatment samples, we found *FGFR1* amplifications in 15% (9/60), *FGFR2* amplifications in 5% (3/60), *FGFR2* activating mutations in 3.3% (2/60), and *FGF3* amplifications in 28.3% (17/60) – for a total of 40% (24/60) of the cohort with at least one alteration in one of these three genes (Fig.2A). Overall, the prevalence of

FGFR1, *FGFR2*, and *FGF3* alterations in the resistant metastatic setting seen here is increased compared to what was observed in previously published cohorts of primary ER+ breast cancer, such as The Cancer Genome Atlas (TCGA) [29], and comparable to other datasets of metastatic ER+ breast cancer (Supplemental Table.3). The incidence of *FGFR2* alterations (6.7%), in particular, is markedly increased compared to primary treatment-naïve breast cancer, in which the incidence is less than 2% in TCGA (Supplemental Table.3).

To determine if this enrichment of FGFR/FGF alterations in the metastatic setting was due to acquisition/selection under the selective pressure of endocrine therapy, we performed an evolutionary analysis to evaluate clonal structure and dynamics, including changes in mutations and copy number for the 24 patients harboring FGFR/FGF alterations. For this analysis, we define “acquired” alterations as alterations with higher representation in the post-treatment sample as compared to the pre-treatment sample (see Methods). Although we use the term “acquired”, we recognize that when the mutation is not detected in the pre-treatment sample, we cannot distinguish between pre-existing alteration that was selected for and clonally enriched versus *de novo* alterations that developed during the treatment.

In 12 of the 24 patients with FGFR or FGF alterations (50%), the alterations were acquired in the post-treatment sample as compared to the pre-treatment sample (Fig. 2A, marked in red). Five out of nine *FGFR1* amplifications were acquired (55.6%), while all four *FGFR2* alterations were acquired (100%), including one patient (Pt 0300350) with

acquisition of both an *FGFR2* mutation and amplification. *FGF3* amplifications were acquired in 4 of 17 tumors (23.5%), including one case in which an *FGFR1* amplification was co-acquired. The concurrent acquisition may suggest that the evolutionary selection of both the ligand and receptor provided additional fitness in this tumor. Among the other 12 patients, the alterations in eight patients were shared in both pre-treatment and post-treatment samples (Fig 2A, marked in black), and evolutionary status of alterations in the remaining four patients was inconclusive (Fig 2A, marked in grey). The increase in copy number (corrected for tumor purity and ploidy, Supplemental Table.4) from pre-treatment to post-treatment for *FGFR1*, *FGFR2*, and the *FGF3* amplicon in all 12 patients is depicted in Fig.2B.

Two of the acquired alterations found in these 12 patients were single nucleotide variants (SNVs) in the *FGFR2* gene: M538I and N550K. N550K is the most common *FGFR2* mutation in breast cancer while M538I was previously identified in lung cancer but has not yet been characterized in breast cancer [30]. Figure 2C illustrates the change in the estimated fraction of tumor cells harboring each genomic alteration (CCF) from the pre-treatment biopsy to the resistant biopsy. In both patients, the *FGFR2* mutations were either not detected in the primary tumor (N550K in Pt 0300350) or detected in a small fraction (CCF of 2%) of the pre-treatment tumor (M538I in Pt 0300348). In both patients the activating *FGFR2* mutations in the post-treatment biopsies were clonally acquired (CCF of 100%) (Fig.2B).

Notably, the acquired alterations in *FGFR1*, *FGFR2*, and *FGF3* were largely mutually exclusive with acquired *ESR1* mutations and *HER2* mutations (Fig.2A). *ESR1* mutations are the most common mechanism described for acquired endocrine resistance [31]. Although the overall rate of acquired *ESR1* mutation in this cohort is 22% (13/60), among the 12 cases of acquired FGFR and FGF alterations, only one patient also has an acquired *ESR1* mutation (Fig. 2A). Similarly, only one of these 12 patients had acquired a *HER2* mutation *ERBB2 I628M* (which was an alteration of unknown significance), suggesting that these are also mutually exclusive mechanisms of resistance.

Although we highlight *FGF3* as the key gene in the amplicon (given the results of the gain-of-function screen), *FGF3* resides in genomic proximity to *FGF4*, *FGF19* and *CCND1* and these four genes are often co-amplified. Here, in 3 out of the 4 cases with acquired *FGF3* amplification, *FGF3* copies were gained without co-acquisition of *CCND1* amplification, suggesting that this acquisition can occur as an independent genomic event (Supplemental Data Fig.S4). Similarly, 2 out of the 4 cases with acquired *FGF3* did not have co-acquisition of *FGF19* amplification. In all 4 of the cases with *FGF3* amplification, *FGF4* was also co-amplified. The other concurrent genetic alterations for the 12 patients with acquired FGFR/FGF alterations are shown in Supplemental Data Fig.S5 and Supplemental Table.5-6.

Figure 3 depicts clinical vignettes for six of the patients with acquired *FGFR1*, *FGFR2*, and/or *FGF3* alterations in their post-treatment biopsies. All patients were treated with ER-directed therapy before acquiring FGF or FGFR alterations, including tamoxifen (3

patients), AIs (6 patients), and fulvestrant (3 patients). Vignettes for the other six patients with acquired *FGFR1*, *FGFR2*, and/or *FGF3* alterations in their post-treatment biopsies are shown in Supplemental Data Fig.S6A. Detailed clinicopathological features and therapy details for all 12 patients are found in Supplemental Table.7.

In addition to these 12 patients in our cohort, we identified several additional patients with acquired activating mutations in *FGFR1*(N546K) and *FGFR2* (N550K, K660N) following the development of resistance to endocrine therapy (Supplemental Data Fig.S6B and Supplemental Table.8).

In summary, we observed acquired alterations in *FGFR1*, *FGFR2*, or *FGF3* in 20% (12/60) of patients with endocrine resistant ER+ MBC – comparable to the known frequency of acquired mutations in *ESR1* – highlighting the important role of the FGFR pathway in acquired resistance to ER-directed therapies.

Active FGFR signaling leads to resistance to SERDs through activation of the MAP kinase pathway

To further investigate how FGFR/FGF genes may confer resistance to ER-directed therapy, we treated T47D cells with FGF3, FGF6, FGF10 or FGF22 ligand. Each of these ligands resulted in resistance to fulvestrant (Fig.4A). This effect was reversed by PD173074, a pan-FGFR inhibitor (Fig.4A). The addition of these FGF ligands enhanced phosphorylation of ERK and AKT, which was reversed by PD173074 (Supplemental

Data Fig.S7A). FGF3, FGF6, FGF10 and FGF22 also reduced fulvestrant sensitivity in MCF7 cells (Supplemental Data Fig. S7B-C).

We next overexpressed FGFR1, FGFR2, or GFP in T47D cells through lentiviral transduction and examined the impact on susceptibility to SERDs. Overexpression of FGFR1 or FGFR2 alone did not affect sensitivity to fulvestrant. However, with the addition of FGF2 ligand, both FGFR1 and FGFR2 rendered cells highly resistant to fulvestrant (Fig. 4B). A similar resistance phenotype was also observed when T47D cells expressing FGFR1 or FGFR2 were treated with GDC-0810 or tamoxifen (Supplemental Data Fig.S8 A-C). In comparison, FGF2 ligand alone reduced sensitivity to SERDs in control cells expressing GFP to a much lesser extent than in the FGFR1 or FGFR2 expressing cells, suggesting the potent resistance phenotype requires both FGF ligand and receptor. This requirement for the presence of both FGF ligand and receptor for maximal resistance phenotype may also explain why only FGFs but not FGFR1 or FGFR2 scored in the resistance screen (Fig.1 A-B). The resistance phenotype resulting from FGFR1 and FGFR2 overexpression was completely reversed by the addition of PD173074 (Fig. 4B). Similar results were obtained in MCF7 cells (Supplemental Data Fig.S8 E-F).

FGFR1 and FGFR2 overexpression (in the presence of FGF2 ligand) induced more potent phosphorylation of AKT and ERK than the GFP control, which was reversed by PD173074 (Fig.4C and Supplemental Data Fig. S8 D and G). These results are consistent with previous findings that FGFR1 activation led to MAPK activation and fulvestrant

resistance [32]. Collectively, these findings suggest that FGFR1 and FGFR2 cause SERD resistance through the activation of MAPK and/or PI3K/AKT pathways.

We examined the sensitivity of cells overexpressing FGFR1 or FGFR2 to several inhibitors of downstream effectors: the MEK inhibitor trametinib, the AKT inhibitor AZD5363, and the mTOR inhibitor everolimus. FGFR1 or FGFR2 overexpression in the presence of FGF2 led to hypersensitivity to trametinib (Supplemental Data Fig.S9A), but reduced sensitivity to AKT and mTOR inhibitors (Supplemental Data Fig.S9A).

We attempted to reverse FGFR-induced resistance to fulvestrant by inhibiting the MAPK pathway. Treatment of FGFR1 overexpressing cells with trametinib partially resensitized cells to fulvestrant, and treatment of FGFR2 overexpressing cells with trametinib fully resensitized the cells to fulvestrant (Fig.4D). In contrast, trametinib did not reverse an increase in viability induced by FGF2 in the GFP control cells. This is likely because FGF2 alone may not sufficiently increase MAPK signaling to induce a dependency, which is consistent with much lower sensitivity to trametinib in GFP cells as compared to FGFR1 and FGFR2 cells in the presence of FGF2 (Supplemental Data Fig.S9A and B). Colony formation assays produced similar results (Supplemental Data Fig.S9C). Treatment with the mTOR inhibitor everolimus also partially reversed resistance conferred by FGFR1 or FGFR2 overexpression (Supplemental Data Fig.S9D). Together, these results suggest that the MAPK pathway is the primary downstream effector of FGFR activation resulting in endocrine resistance.

FGFR activation confers cross-resistance to CDK4/6 inhibitors

Since the combination of endocrine therapy and CDK4/6 inhibitors is now a standard of care treatment for patients with ER+ metastatic breast cancer, we also examined the effect of FGFR signaling on sensitivity to the combination of fulvestrant and the CDK4/6 inhibitor palbociclib. In T47D cells, FGFR1 and FGFR2 overexpression in the presence of FGF2 also conferred resistance to combination treatment of fulvestrant and palbociclib. Resistance to fulvestrant and palbociclib was abrogated by PD173074 and also partially reversed by trametinib (Fig. 4D and Supplemental Data Fig. S9E), further providing the support for the role of MAPK pathway activation in FGFR-mediated drug resistance. The reversal of resistance by trametinib was accompanied by reduced ERK phosphorylation (Fig. 4E). Similar results were achieved in MCF7 cells, although everolimus was more effective than trametinib in reversing the resistance phenotype by FGFR1 or FGFR2 overexpression in this cell line (Supplemental Data Fig.S10). In the presence of fulvestrant and palbociclib, FGFR1 or FGFR2 overexpression was accompanied by increased p-Rb and CCND1 levels, both of which were partially reversed by trametinib (Fig.4E). This is consistent with prior results suggesting that CCND1 was involved in FGF2-mediated drug resistance [33].

Clinical evidence also supports the finding that FGFR alterations can cause resistance to CDK4/6 inhibitors. Following the acquisition of *FGFR2* N550K (along with *FGFR2* amplification), Pt 0300350 did not respond to the combination of letrozole and palbociclib (Fig.3), suggesting that *FGFR2* alterations may lead to intrinsic resistance to the combination of endocrine therapy and CDK4/6 inhibitors. Another patient with an

FGFR2 N550K mutation (FM Patient 2) also did not respond to the combination of fulvestrant and palbociclib (Supplemental Data Fig.S6B). Collectively, this suggests targeting the *FGFR* pathway may also be a viable strategy to overcome *FGFR/FGF*-mediated resistance to SERDs and CDK4/6 inhibitors.

FGFR2 mutations found in patients are activating with differential sensitivity to FGFR inhibitors

We identified 3 acquired mutations in the kinase domain of *FGFR2* in patients who developed resistance to endocrine therapy. Two of these, *FGFR2* N550K and K660N, are known activating *FGFR2* mutations that have been previously identified in breast cancer [30, 34]. The third mutation, *FGFR2* M538I, has not been previously reported in breast cancer, but was identified through *in vitro* screening as a reversible pan *FGFR* inhibitor resistance mutation and confirmed to increase kinase activity *in vitro* [35] (Fig.5A).

We expressed all three *FGFR2* kinase domain mutants in T47D cells through lentiviral transduction, as well as wildtype (WT) *FGFR2* and GFP as negative controls. All three mutants elicited higher kinase activity than WT *FGFR2* constitutively, demonstrated by levels of p-FRS2 (a direct substrate for *FGFR2*), p-ERK and p-AKT (Fig.5B). The addition of FGF2 ligand further enhanced downstream signaling for all *FGFR2* mutants, and the enhanced signaling was blocked by PD173074 for *FGFR2* M538I and K660N, but not for N550K (Fig.5B). *FGFR2* mutants were also expressed under a tetracycline responsive promoter in T47D cells grown in low doses of doxycycline to determine the functionality at lower expression levels. All three *FGFR2* mutations acquired in breast

cancer patients are functionally active – FGFR2 N550K is constitutively active while FGFR2 M538I and K660N may be more ligand-dependent at low levels of expression (Supplemental Data Fig.S11A).

All 3 FGFR2 mutants led to modest resistance to fulvestrant or the combination of fulvestrant and palbociclib (Fig.5C), which was enhanced in the presence of FGF2 ligand. PD173074 reversed the resistance phenotype for cells overexpressing FGFR2 M538I and FGFR2 K660N as well as WT FGFR2 to fulvestrant, but not cells overexpressing FGFR2 N550K (Fig.5C). Similar results were obtained in MCF7 cells (Supplemental Data Fig.S12).

Activating FGFR2 mutations can be targeted with irreversible FGFR inhibitors

Because of the differential responses of these FGFR2 mutants to PD173074, we tested the ability of additional FGFR inhibitors to resensitize cells expressing these mutants to fulvestrant. FIIN-2 and FIIN-3 are two irreversible covalent pan-FGFR inhibitors that target a cysteine conserved in FGFR1-4 and have exquisite selectivity for some FGFR2 mutations including M538I and K659N [36]. In addition, AZD4547 is a selective FGFR inhibitor that was previously shown to inhibit FGFR2 N550K [37].

Both FIIN-2 and FIIN-3 were more effective in inhibiting the downstream signaling (p-FRS2, p-ERK and p-AKT) induced by FGFR2 N550K as compared to PD173074 and AZD4547 (Fig.5D), with FIIN-3 being more potent than FIIN-2 (Supplemental Data Fig.S13). T47D cells stably overexpressing FGFR2 mutant were exquisitely sensitive to

FIIN-2 and FIIN-3 as compared to cells expressing GFP or FGFR2 WT (Supplemental Data Fig.S11B). While resistance to WT FGFR1/2 and FGFR2 M538I and FGFR2 K660N can be reversed by multiple FGFR inhibitors, for some mutants like FGFR2 N550K, only the irreversible pan-FGFR inhibitors FIIN-2 and FIIN-3 successfully resensitized cells to fulvestrant (Fig.5E), highlighting the fact that specific resistance mutations might require different strategies to overcome or preempt endocrine resistance.

Transcriptional changes induced by FGFR/FGF include ER reprogramming and MAPK activation

To examine transcriptional changes associated with FGFR pathway activation, we performed RNA-Seq on T47D cells overexpressing FGFR1, FGFR2 (wildtype), FGFR2 activating mutants (M538I, N550K, K660N), or FGF3, as well as on GFP and parental lines as controls (Supplemental Table.9). We combined these profiles with transcriptional profiles we previously generated [11] from of T47D cells overexpressing wildtype and kinase-dead HER2, HER2 activating mutants (S653C, L755S, V777L and L869R), and ESR1 Y537S, for a total of 15 genetic perturbations examined.

Linear discriminant analysis of these profiles indicated that samples from cells overexpressing FGFR1, wildtype FGFR2, FGFR2 activating mutants, FGF3, wildtype HER2, or HER2 activating mutants are separated from controls (parental cells, GFP expressing, or kinase-dead HER2 D845A) along the first LD component (LD1), as well as from a separate group of cells overexpressing mutant ESR1 along the second LD component (LD2), indicating a common receptor tyrosine kinase (RTK)/growth factor-

driven cell state that is distinct from the mutant ER state (Fig. 6A). Along LD1, the cells overexpressing FGF3 have distinct scores from those overexpressing FGFR (p.value = 2.12×10^{-10} , Welch's t-test), suggesting that in our model system, FGF ligand overexpression is different from FGFR overexpression (Fig. 6A). The overall signature strength of RTKs and growth-factor signaling genes (defined in Supplemental Methods and shown in Supplemental Table.10) were highly correlated with scores on LD1 (Spearman's rho= 0.926), suggesting that LD1 broadly represents RTK and growth-factor pathway activation.

Using differential expression analysis to compare activating constructs with GFP and parental controls, we defined transcriptional signatures for all FGFR1/2 constructs (FGFR1/2), FGF3, and all HER2 activating mutants (HER2-MUT). Comparison of the top 200 highly expressed genes in each of the FGFR1/2, FGF3, and HER2-MUT signatures (Supplemental Table.11) highlights the high degree of similarity between these groups, with 32 genes common to the FGFR1/2 and FGF3 signatures (Odds-ratio=39.63 p.value= 4.7×10^{-37} , two-sided Fisher's exact test), 84 genes common to the FGFR1/2 and HER2-MUT signatures (Odds-ratio=219.4, p.value= 1.025×10^{-140} , two-sided Fisher's exact test), and 18 upregulated genes common to all 3 groups (Supplemental Data Fig.S14A).

We next defined an FGF/R-ACT transcriptional state based on 377 genes that are upregulated in FGF3 and FGFR1/2 cell lines compared with controls (Fig. 6B and Supplemental Table.10). Gene set enrichment analysis [38] of the FGF/R-ACT state vs.

5,150 previously characterized gene sets (Supplemental Table.12) demonstrated that the shared FGF/R-ACT state is enriched for upregulation of RTK/growth factor receptors signaling, RAS/MAPK signaling, and growth factor–induced ER target genes (Fig. 6C), similar to what we have previously shown for HER2 activating mutants [11]. This is consistent with a model in which FGFR/FGF activation leads to ER reprogramming via MAPK pathway activation, potentially shifting the transcriptional spectrum from genes activated by transcription factor AF2 to those activated by AF1. Of note, the genes associated with mTOR signaling were variably upregulated and downregulated in FGF/R-ACT state (Fig. 6C), suggesting only moderate mTOR activation as compared to the robust MAPK activation signal observed. Similar transcriptional signatures were seen when the FGF/R-ACT signature was characterized under fulvestrant treatment, demonstrating that the FGF/R-ACT state is present even when ER signaling is inhibited, consistent with the phenotype of fulvestrant resistance (Supplemental Table.11-12).

Next, we evaluated the effect of ten different drug combinations on the transcriptional signatures in FGFR/FGF expressing cell lines and control cells profiled by RNA-seq. The activated RAS/MAPK signature, ER signaling driven by growth factors signature, and FGF/R-ACT signature present in cells overexpressing FGFR/FGF constructs persisted under treatment with fulvestrant, palbociclib, or their combination (Fig. 6D and Supplemental Data Fig.S14B-C). Treatment with FIIN-3, alone or in combination with fulvestrant and/or palbociclib largely reversed the activation of all three signatures (Supplemental Table.13). Effective suppression of all three signatures was also achieved

by trametinib plus fulvestrant, with or without palbociclib (Fig. 6D and Supplemental Data Fig. S14B-C; Supplemental Table 13),

Targeting MAPK pathway via SHP2 inhibition can overcome FGFR-induced endocrine resistance

Data from the gain-of-function ORF screen, the transcriptomic analysis, and our individual *in vitro* experiments together suggest that MAPK pathway may represent a common node for drug resistance in ER+ metastatic breast cancer. FGFR2 mutants, in particular, rendered cells more sensitive to trametinib than did GFP or WT FGFR2 (Supplemental Data Fig.S14D), further supporting the finding that FGFR signaling requires the MAPK pathway in this context. Src homology phosphotyrosyl phosphatase 2 (SHP2) is protein downstream of RTKs that is required for RAS activation. Several recent studies have demonstrated that co-targeting SHP2 prevented adaptive resistance to MEK inhibition in multiple RAS-driven cancer models [39-41]. Consistent with this, cell lines expressing FGFR2 mutants were hypersensitive to the SHP2 inhibitor SHP099 (Supplemental Data Fig.S14E). We next examined the ability of combinations of SHP099, trametinib, fulvestrant, and/or palbociclib to overcome resistance in FGFR-expressing cell lines. Similar to trametinib, SHP099 as a single agent partially rescued resistance to fulvestrant and/or palbociclib conferred by FGFR1, and completely rescued resistance conferred by FGFR2. Cells expressing the FGFR2 constructs (wildtype or activating mutations) were particularly sensitive to the treatment regimen of trametinib and SHP099 in addition to fulvestrant and palbociclib (Fig.6E-F), in comparison with minimal inhibitory effect of MEK and SHP2 inhibition in GFP control cells. These

results suggest that targeting MEK and SHP2 may serve as an even more effective strategy to overcome multiple forms of FGFR pathway mediated resistance to endocrine therapy and CDK4/6 inhibitors in MBC, as well as, potentially, other RTK-induced mechanisms of resistance.

Discussion

Taken together, our results from genome-scale gain-of-function screen and genomic profiling of patient samples suggest that activating FGFR pathway alterations are a distinct mechanism of acquired resistance to multiple forms of ER-directed therapy in MBC that can be overcome by FGFR and/or MAPK pathway inhibitors.

Our findings are consistent with two recently published studies. Formisano, Arteaga, and colleagues identified *FGFR1* amplification as a mechanism of resistance to CDK4/6 inhibitors [42]. In this study, FGFR1 knockdown sensitized FGFR1-amplified CAMA-1 cells to fulvestrant/palbociclib, and the addition of FGFR inhibitor erdafitinib to fulvestrant/palbociclib further induced tumor regression in patient-derived xenografts. In another study, Drago et al. demonstrated that FGFR1 amplification confers resistance to ER, PI3K and CDK4/6 inhibitors while retaining TORC sensitivity [43]. Our results extend our understanding of endocrine resistance with multiple novel findings-identifying novel pathways and genes associated with endocrine resistance by functional screen, demonstrating the acquisition of multiple FGFR pathway alterations after the development of resistance to endocrine therapy and/or CDK4/6 inhibitors in matched tumor samples, and highlighting therapeutic agents that can overcome this resistance.

Our genome-scale screen provided a comprehensive view into the resistance mechanisms to SERDs. Similar resistance genes were nominated for fulvestrant and GDC-0810, thereby confirming the two drugs have similar mechanism of action. Of note, two ESR1 ORFs conferred resistance specifically to GDC-0810 but not fulvestrant, possibly due to GDC-0810 having a less potent effect on ER degradation than fulvestrant [21, 44].

Among the resistance mechanisms shared by fulvestrant and GDC-0810, many are frequently altered in ER+ MBC, such as *CCNDs/CDK6*, *KRAS/MAPK*, *EGFR/ERBB2* and *PIK3CA/AKTs/PIMs*, and agents targeting those alterations are under clinical development to be combined with endocrine therapy [14, 45]. We also identified potential resistance mechanisms that are not characterized to the same extent, such as G protein-coupled receptors, Wnt pathway (*FZD10*, *RSPO1*, *RSPO3*) and Src family kinases (*YES1*, *FYN*, *FGR*), providing clues as to the potential crosstalk between these pathways and ER signaling [46-48] and suggesting that breast cancer patients harboring functional alterations in these pathways may develop resistance to SERDs. We recognize that those screens were performed using cell lines as model system, and the results will need to be further validated in the clinical setting. We have provided the full genome-scale screen data as a resource to the community of researchers interested in resistance to ER-directed therapies as well as the biology of estrogen receptor dependencies in ER+ breast cancer.

Our ultimate goal is to identify resistance mechanisms that are clinically relevant and can be therapeutically targeted. By comparing paired pre-treatment and post-treatment

tumors, our evolutionary analyses identified acquired *FGFR1* and *FGFR2*, and *FGF3* alterations in 12 out of 60 post-treatment samples, further highlighting a potential role for the FGFR pathway in driving drug resistance and disease progression. Most notably, all four alterations in *FGFR2* in our cohort were found to be acquired after the development of resistance to endocrine therapy. Our overall findings are consistent with other recent studies which noted some patients with acquired *FGFR1* and *FGFR2* alterations following treatment of endocrine therapy [42, 43, 49, 50], and provides a mechanistic explanation for these acquisitions.

This analysis was enabled by a novel method we developed to compare the magnitude of amplification in matched pre- and post-treatment samples while considering key confounders to allow for more reliable assignment of copy gain or loss. Since matched tumor samples of the same patient are highly variable in the cancer cell fraction (purity) and often variable in ploidy, we computed the purity-corrected copy number above ploidy and set a relatively stringent threshold of changes in CNAP to define acquired amplification (see Methods), as cancer clones bearing amplifications with high focality and magnitude in *FGFR/FGF* genes are more likely to induce dependency on FGFR pathway and result in endocrine resistance.

Our genomic analysis has some limitations and caveats. The observed alterations may not exclusively result from endocrine therapy as some patients received other therapies between the two collected biopsies. Moreover, tumors with *FGFR/FGF* alterations also harbor alterations in other cancer genes, which may contribute to drug resistance as well

(Supplemental Data Fig.S5 and Supplemental Table.5). Despite these caveats, with the evidence from unbiased screens, genomic evidence in relevant patient samples, and confirmatory experimental models, the FGFR pathway clearly emerges as a clinically important resistance mechanism for SERDs and CDK4/6 inhibitors.

Strategies to target the FGFR pathway in breast cancer patients with FGFR alterations are currently being assessed in clinical trials [51-56]. The combination of FGFR inhibitors and endocrine therapy is also being clinically investigated [51]. As FGFR pathway activation also results in resistance to CDK4/6 inhibitors, a triple combination with the addition of CDK4/6 inhibitors may also be considered. One challenge for the use of FGFR inhibitors is to identify reliable biomarkers. Our results suggest focal and high level amplifications, clonal activating mutations or high expression levels of FGFR and FGF genes, particularly in the metastatic setting, may be used to guide the clinical use of FGFR inhibitors. Activating alterations in *FGFR2*, which are rare in primary treatment naïve breast cancer but appear to be clonally acquired in a subset of patients with resistant ER+ MBC, may be a particularly good biomarker for the development of FGFR inhibitors.

Our work also highlights that the effective clinical use of FGFR inhibitors needs to consider the variable drug sensitivity of different FGFR2 mutations, which were acquired in some patients following endocrine therapy. The two irreversible pan-FGFR kinase inhibitors, FIIN-2 and FIIN-3, had superior efficacy in targeting all FGFR2 mutants including N550K when compared to other FGFR inhibitors. Both FIIN compounds

exhibits good overall kinase selectivity at the concentration of 1 μ M, although FIIN-3 can also target wildtype and several mutant EGFR [36]. The *in vivo* efficacy, other off-target effects and toxicity of FIIN compounds still warrant further investigation.

Alterations in FGFR1 and FGFR2 activated the MAPK pathway, and MEK inhibition was able to overcome the resistance conferred by FGFR pathway to some degree. We previously demonstrated acquired ERBB2 mutations resulted in a reprogrammed ER signature and an elevated MAPK transcriptional signature [11]. In this study, the transcriptional analysis results suggest that MAPK activation resulting from FGFR/FGF overexpression is more pronounced than mTOR activation. This is consistent with our experimental findings, which demonstrated that MAPK inhibition is particularly effective in cells expressing FGFR2 activating alterations. Furthermore, increased frequency of alterations in MAPK pathway genes have been found in tumors post hormonal therapy, including *EGFR*, *ERBB2* and *NF1* [14]. The fact that multiple mechanisms of resistance to ER-directed therapies and/or CDK4/6 inhibitors activate the MAPK pathway suggests that this may be an important node of resistance in ER+ MBC. Thus, combining endocrine therapy and CDK4/6 inhibitors with agents that target MAPK pathway, such as MEK inhibitors and/or SHP2 inhibitors [57, 58], may be a unifying strategy to overcome or prevent resistance resulting from multiple genetic aberrations that lead to resistance in ER+ MBC. Further *in vivo* validation is needed to establish the translational implication of the combinational strategies proposed herein.

In summary, the integration of a functional genomic screen and genomic analysis of pre- and post-treatment biopsies revealed the FGFR pathway as an important resistance mechanism for endocrine therapy and CDK4/6 inhibitors in ER+ breast cancer. With the increasing use of SERDs and CDK4/6 inhibitors in the clinic, we anticipate that the prevalence of FGFR/FGF alterations might increase in the future. Targeting the FGFR pathway with FGFR inhibitors or agents that target downstream MAPK signaling may improve clinical outcomes in patients with aberrations in FGFR/FGF genes. Furthermore, our study highlights the need to sequence metastatic biopsy or blood biopsies at the time of resistance to identify patients with these alterations who may benefit from targeting the FGFR pathway.

Data availability

Tumor and germline whole exome sequencing data generated and analyzed for this study have been deposited in the access-controlled public repository dbGAP with accession code phs001285 (<https://www.ncbi.nlm.nih.gov/gap>). RNA-seq data are available through GEO under accession GSE153509. Additional data generated in this study including tumor exome analysis and RNA-seq data are available within the paper and in the supplementary information files.

Acknowledgements

We thank Qaren Quartey, Christian Kapstad and Gabriela Johnson for technical assistance; Karla Helvie, Laura Dellostritto, Lori Marini, Nelly Oliver, Shreevidya Periyasamy, Colin Mackichan, Max Lloyd, and Mahmoud Charif for assistance with patient sample collection and annotation; and Flora Luo, Tinghu Zhang and Nathanael Gray for providing reagents. We thank Jorge Gómez Tejeda Zañudo for helpful discussions and comments on the manuscript. We are grateful to all the patients who volunteered for our tumor biopsy protocol and generously provided the tissue analyzed in this study.

Grant support

This work was supported by the Department of Defense W81XWH-13-1-0032 (N.W.), NCI Breast Cancer SPORE at DF/HCC #P50CA168504 (N.W., N.U.L and E.P.W), Susan G. Komen CCR15333343 (N.W.), The V Foundation (N.W.), The Breast Cancer Alliance (N.W.), The Cancer Couch Foundation (N.W.), Twisted Pink(N.W.),Hope

Scarves (N.W.), Breast Cancer Research Foundation (N.U.L. and E.P.W.), ACT NOW (to Dana-Farber Cancer Institute Breast Oncology Program), Fashion Footwear Association of New York (to Dana-Farber Cancer Institute Breast Oncology Program), Friends of Dana-Farber Cancer Institute (to N.U.L.), Stand Up to Cancer (N.W.), National Science Foundation (N.W.), and SU2C-TVF Convergence Scholarship (P.M.). Research supported by the 2013 Landon Foundation-AACR INNOVATOR Award for Research in Personalized Cancer Medicine, Grant Number 13-60-27-WAGL (N.W.). Research supported by the 2017 AACR Basic Cancer Research Fellowship, Grant Number 17-40-01-MAP (P.M.).

Author contributions

P.M., O.C. and N.W. conceived and designed the study; P.M. K.K. and J.K. performed experiments; O.C. and J.B. performed the computational analyses with input from S.F.; P.E., S.A.W., A.G.W., and N.W. performed clinical data abstraction and annotation; P.M. and M.S.C performed the RNA sequencing experiments; O.R. helped with the execution of the RNA-Seq; A.R. helped with the RNA-Seq data analysis; U.N. performed the prior HER2 mutant RNA sequencing experiments; J.C., V.M., and M.C. provided the clinical and genomic data for the 3 patients in the Foundation Medicine cohort; F.P and D.R. helped with the design and execution of the ORF screen; E.P.W., N.U.L., and N.W. oversaw patient enrollment and sample collection on the metastatic biopsy protocol; P.M., O.C. and N.W. wrote the manuscript with input from all authors; N.W. supervised the study.

References

1. Chen WY, Colditz GA: **Risk factors and hormone-receptor status: epidemiology, risk-prediction models and treatment implications for breast cancer.** *Nature clinical practice Oncology* 2007, **4**(7):415-423.
2. Osborne CK, Schiff R: **Mechanisms of endocrine resistance in breast cancer.** *Annual review of medicine* 2011, **62**:233-247.
3. Lei JT, Gou X, Ellis MJ: **ESR1 fusions drive endocrine therapy resistance and metastasis in breast cancer.** *Molecular & cellular oncology* 2018, **5**(6):e1526005.
4. Robinson DR, Wu YM, Vats P, Su F, Lonigro RJ, Cao X, Kalyana-Sundaram S, Wang R, Ning Y, Hodges L *et al*: **Activating ESR1 mutations in hormone-resistant metastatic breast cancer.** *Nature genetics* 2013, **45**(12):1446-1451.
5. Toy W, Shen Y, Won H, Green B, Sakr RA, Will M, Li Z, Gala K, Fanning S, King TA *et al*: **ESR1 ligand-binding domain mutations in hormone-resistant breast cancer.** *Nature genetics* 2013, **45**(12):1439-1445.
6. Merenbakh-Lamin K, Ben-Baruch N, Yeheskel A, Dvir A, Soussan-Gutman L, Jeselsohn R, Yelensky R, Brown M, Miller VA, Sarid D *et al*: **D538G mutation in estrogen receptor-alpha: A novel mechanism for acquired endocrine resistance in breast cancer.** *Cancer Res* 2013, **73**(23):6856-6864.
7. Jeselsohn R, Yelensky R, Buchwalter G, Frampton G, Meric-Bernstam F, Gonzalez-Angulo AM, Ferrer-Lozano J, Perez-Fidalgo JA, Cristofanilli M, Gomez H *et al*: **Emergence of constitutively active estrogen receptor-alpha mutations in pretreated advanced estrogen receptor-positive breast cancer.** *Clin Cancer Res* 2014, **20**(7):1757-1767.
8. Garcia-Becerra R, Santos N, Diaz L, Camacho J: **Mechanisms of resistance to endocrine therapy in breast cancer: focus on signaling pathways, miRNAs and genetically based resistance.** *International journal of molecular sciences* 2012, **14**(1):108-145.
9. Miller TW, Perez-Torres M, Narasanna A, Guix M, Stal O, Perez-Tenorio G, Gonzalez-Angulo AM, Hennessy BT, Mills GB, Kennedy JP *et al*: **Loss of Phosphatase and Tensin homologue deleted on chromosome 10 engages ErbB3 and insulin-like growth factor-I receptor signaling to promote antiestrogen resistance in breast cancer.** *Cancer Res* 2009, **69**(10):4192-4201.

10. Massarweh S, Osborne CK, Jiang S, Wakeling AE, Rimawi M, Mohsin SK, Hilsenbeck S, Schiff R: **Mechanisms of tumor regression and resistance to estrogen deprivation and fulvestrant in a model of estrogen receptor-positive, HER-2/neu-positive breast cancer.** *Cancer Res* 2006, **66**(16):8266-8273.
11. Nayar U, Cohen O, Kapstad C, Cuoco MS, Waks AG, Wander SA, Painter C, Freeman S, Persky NS, Marini L *et al*: **Acquired HER2 mutations in ER(+) metastatic breast cancer confer resistance to estrogen receptor-directed therapies.** *Nature genetics* 2018.
12. Croessmann S, Formisano L, Kinch LN, Gonzalez-Ericsson PI, Sudhan DR, Nagy RJ, Mathew A, Bernicker EH, Cristofanilli M, He J *et al*: **Combined Blockade of Activating ERBB2 Mutations and ER Results in Synthetic Lethality of ER+/HER2 Mutant Breast Cancer.** *Clin Cancer Res* 2019, **25**(1):277-289.
13. Sokol ES, Feng YX, Jin DX, Basudan A, Lee AV, Atkinson JM, Chen J, Stephens PJ, Frampton GM, Gupta PB *et al*: **Loss of function of NF1 is a mechanism of acquired resistance to endocrine therapy in lobular breast cancer.** *Ann Oncol* 2019, **30**(1):115-123.
14. Razavi P, Chang MT, Xu G, Bandlamudi C, Ross DS, Vasani N, Cai Y, Bielski CM, Donoghue MTA, Jonsson P *et al*: **The Genomic Landscape of Endocrine-Resistant Advanced Breast Cancers.** *Cancer cell* 2018, **34**(3):427-438 e426.
15. Johannessen CM, Johnson LA, Piccioni F, Townes A, Frederick DT, Donahue MK, Narayan R, Flaherty KT, Wargo JA, Root DE *et al*: **A melanocyte lineage program confers resistance to MAP kinase pathway inhibition.** *Nature* 2013, **504**(7478):138-142.
16. Wilson FH, Johannessen CM, Piccioni F, Tamayo P, Kim JW, Van Allen EM, Corsello SM, Capelletti M, Calles A, Butaney M *et al*: **A functional landscape of resistance to ALK inhibition in lung cancer.** *Cancer cell* 2015, **27**(3):397-408.
17. Le X, Antony R, Razavi P, Treacy DJ, Luo F, Ghandi M, Castel P, Scaltriti M, Baselga J, Garraway LA: **Systematic Functional Characterization of Resistance to PI3K Inhibition in Breast Cancer.** *Cancer discovery* 2016, **6**(10):1134-1147.
18. Gonzalez-Malerva L, Park J, Zou L, Hu Y, Moradpour Z, Pearlberg J, Sawyer J, Stevens H, Harlow E, LaBaer J: **High-throughput ectopic expression screen for tamoxifen resistance identifies an atypical kinase that blocks autophagy.** *Proceedings of the National Academy of Sciences of the United States of America* 2011, **108**(5):2058-2063.
19. Fox EM, Miller TW, Balko JM, Kuba MG, Sanchez V, Smith RA, Liu S, Gonzalez-Angulo AM, Mills GB, Ye F *et al*: **A kinome-wide screen identifies**

- the insulin/IGF-I receptor pathway as a mechanism of escape from hormone dependence in breast cancer.** *Cancer research* 2011, **71**(21):6773-6784.
20. Mendes-Pereira AM, Sims D, Dexter T, Fenwick K, Assiotis I, Kozarewa I, Mitsopoulos C, Hakas J, Zvelebil M, Lord CJ *et al*: **Genome-wide functional screen identifies a compendium of genes affecting sensitivity to tamoxifen.** *Proceedings of the National Academy of Sciences of the United States of America* 2012, **109**(8):2730-2735.
 21. Joseph JD, Darimont B, Zhou W, Arrazate A, Young A, Ingalla E, Walter K, Blake RA, Nonomiya J, Guan Z *et al*: **The selective estrogen receptor downregulator GDC-0810 is efficacious in diverse models of ER+ breast cancer.** *eLife* 2016, **5**.
 22. Yang X, Boehm JS, Yang X, Salehi-Ashtiani K, Hao T, Shen Y, Lubonja R, Thomas SR, Alkan O, Bhimdi T *et al*: **A public genome-scale lentiviral expression library of human ORFs.** *Nature methods* 2011, **8**(8):659-661.
 23. Adalsteinsson VA, Ha G, Freeman SS, Choudhury AD, Stover DG, Parsons HA, Gydush G, Reed SC, Rotem D, Rhoades J *et al*: **Scalable whole-exome sequencing of cell-free DNA reveals high concordance with metastatic tumors.** *Nature communications* 2017, **8**(1):1324.
 24. Ulz P, Belic J, Graf R, Auer M, Lafer I, Fischereder K, Webersinke G, Pummer K, Augustin H, Pichler M *et al*: **Whole-genome plasma sequencing reveals focal amplifications as a driving force in metastatic prostate cancer.** *Nature communications* 2016, **7**:12008.
 25. Wander SA, Cohen O, Gong X, Johnson GN, Buendia-Buendia JE, Lloyd MR, Kim D, Luo F, Mao P, Helvie K *et al*: **The genomic landscape of intrinsic and acquired resistance to cyclin-dependent kinase 4/6 inhibitors in patients with hormone receptor positive metastatic breast cancer.** *Cancer discovery* 2020.
 26. Barretina J, Caponigro G, Stransky N, Venkatesan K, Margolin AA, Kim S, Wilson CJ, Lehar J, Kryukov GV, Sonkin D *et al*: **The Cancer Cell Line Encyclopedia enables predictive modelling of anticancer drug sensitivity.** *Nature* 2012, **483**(7391):603-607.
 27. Rangel N, Villegas VE, Rondon-Lagos M: **Profiling of gene expression regulated by 17beta-estradiol and tamoxifen in estrogen receptor-positive and estrogen receptor-negative human breast cancer cell lines.** *Breast Cancer (Dove Med Press)* 2017, **9**:537-550.
 28. Cohen O, Kim D, Oh C, Waks A, Oliver N, Helvie K, Marini L, Rotem A, Lloyd M, Stover D *et al*: **Abstract S1-01: Whole exome and transcriptome**

- sequencing of resistant ER+ metastatic breast cancer.** *Cancer Research* 2017, **77**(4 Supplement):S1-01.
29. Cancer Genome Atlas N: **Comprehensive molecular portraits of human breast tumours.** *Nature* 2012, **490**(7418):61-70.
 30. Gallo LH, Nelson KN, Meyer AN, Donoghue DJ: **Functions of Fibroblast Growth Factor Receptors in cancer defined by novel translocations and mutations.** *Cytokine Growth Factor Rev* 2015, **26**(4):425-449.
 31. Jeselsohn R, Buchwalter G, De Angelis C, Brown M, Schiff R: **ESR1 mutations-a mechanism for acquired endocrine resistance in breast cancer.** *Nat Rev Clin Oncol* 2015, **12**(10):573-583.
 32. Turner N, Pearson A, Sharpe R, Lambros M, Geyer F, Lopez-Garcia MA, Natrajan R, Marchio C, Iorns E, Mackay A *et al*: **FGFR1 amplification drives endocrine therapy resistance and is a therapeutic target in breast cancer.** *Cancer Res* 2010, **70**(5):2085-2094.
 33. Shee K, Yang W, Hinds JW, Hampsch RA, Varn FS, Traphagen NA, Patel K, Cheng C, Jenkins NP, Kettenbach AN *et al*: **Therapeutically targeting tumor microenvironment-mediated drug resistance in estrogen receptor-positive breast cancer.** *The Journal of experimental medicine* 2018, **215**(3):895-910.
 34. Reintjes N, Li Y, Becker A, Rohmann E, Schmutzler R, Wollnik B: **Activating somatic FGFR2 mutations in breast cancer.** *PloS one* 2013, **8**(3):e60264.
 35. Byron SA, Chen H, Wortmann A, Loch D, Gartside MG, Dehkhoda F, Blais SP, Neubert TA, Mohammadi M, Pollock PM: **The N550K/H mutations in FGFR2 confer differential resistance to PD173074, dovitinib, and ponatinib ATP-competitive inhibitors.** *Neoplasia* 2013, **15**(8):975-988.
 36. Tan L, Wang J, Tanizaki J, Huang Z, Aref AR, Rusan M, Zhu SJ, Zhang Y, Ercan D, Liao RG *et al*: **Development of covalent inhibitors that can overcome resistance to first-generation FGFR kinase inhibitors.** *Proc Natl Acad Sci U S A* 2014, **111**(45):E4869-4877.
 37. Yu M, Bardia A, Aceto N, Bersani F, Madden MW, Donaldson MC, Desai R, Zhu H, Comaills V, Zheng Z *et al*: **Cancer therapy. Ex vivo culture of circulating breast tumor cells for individualized testing of drug susceptibility.** *Science* 2014, **345**(6193):216-220.
 38. Sergushichev AA: **An algorithm for fast preranked gene set enrichment analysis using cumulative statistic calculation.** *bioRxiv* 2016:060012.
 39. Ahmed TA, Adamopoulos C, Karoulia Z, Wu X, Sachidanandam R, Aaronson SA, Poulikakos PI: **SHP2 Drives Adaptive Resistance to ERK Signaling**

- Inhibition in Molecularly Defined Subsets of ERK-Dependent Tumors.** *Cell reports* 2019, **26**(1):65-78 e65.
40. Fedele C, Ran H, Diskin B, Wei W, Jen J, Geer MJ, Araki K, Ozerdem U, Simeone DM, Miller G *et al*: **SHP2 Inhibition Prevents Adaptive Resistance to MEK Inhibitors in Multiple Cancer Models.** *Cancer discovery* 2018, **8**(10):1237-1249.
 41. Ruess DA, Heynen GJ, Ciecieski KJ, Ai J, Berninger A, Kabacaoglu D, Gorgulu K, Dantes Z, Wormann SM, Diakopoulos KN *et al*: **Mutant KRAS-driven cancers depend on PTPN11/SHP2 phosphatase.** *Nature medicine* 2018, **24**(7):954-960.
 42. Formisano L, Lu Y, Servetto A, Hanker AB, Jansen VM, Bauer JA, Sudhan DR, Guerrero-Zotano AL, Croessmann S, Guo Y *et al*: **Aberrant FGFR signaling mediates resistance to CDK4/6 inhibitors in ER+ breast cancer.** *Nature communications* 2019, **10**(1):1373.
 43. Drago JZ, Formisano L, Juric D, Niemierko A, Servetto A, Wander SA, Spring LM, Vidula N, Younger J, Peppercorn J *et al*: **FGFR1 gene amplification mediates endocrine resistance but retains TORC sensitivity in metastatic hormone receptor positive (HR+) breast cancer.** *Clin Cancer Res* 2019.
 44. Guan J, Zhou W, Hafner M, Blake RA, Chalouni C, Chen IP, De Bruyn T, Giltmane JM, Hartman SJ, Heidersbach A *et al*: **Therapeutic Ligands Antagonize Estrogen Receptor Function by Impairing Its Mobility.** *Cell* 2019, **178**(4):949-963 e918.
 45. AlFakkeh A, Brezden-Masley C: **Overcoming endocrine resistance in hormone receptor-positive breast cancer.** *Curr Oncol* 2018, **25**(Suppl 1):S18-S27.
 46. Loh YN, Hedditch EL, Baker LA, Jary E, Ward RL, Ford CE: **The Wnt signalling pathway is upregulated in an in vitro model of acquired tamoxifen resistant breast cancer.** *BMC Cancer* 2013, **13**:174.
 47. Won HS, Lee KM, Oh JE, Nam EM, Lee KE: **Inhibition of beta-Catenin to Overcome Endocrine Resistance in Tamoxifen-Resistant Breast Cancer Cell Line.** *PloS one* 2016, **11**(5):e0155983.
 48. Vallabhaneni S, Nair BC, Cortez V, Challa R, Chakravarty D, Tekmal RR, Vadlamudi RK: **Significance of ER-Src axis in hormonal therapy resistance.** *Breast cancer research and treatment* 2011, **130**(2):377-385.
 49. Yates LR, Knappskog S, Wedge D, Farmery JHR, Gonzalez S, Martincorena I, Alexandrov LB, Van Loo P, Haugland HK, Lilleng PK *et al*: **Genomic Evolution**

- of Breast Cancer Metastasis and Relapse.** *Cancer cell* 2017, **32**(2):169-184 e167.
50. O'Leary B, Cutts RJ, Liu Y, Hrebien S, Huang X, Fenwick K, Andre F, Loibl S, Loi S, Garcia-Murillas I *et al*: **The Genetic Landscape and Clonal Evolution of Breast Cancer Resistance to Palbociclib plus Fulvestrant in the PALOMA-3 Trial.** *Cancer discovery* 2018, **8**(11):1390-1403.
 51. Musolino A, Campone M, Neven P, Denduluri N, Barrios CH, Cortes J, Blackwell K, Soliman H, Kahan Z, Bonnefoi H *et al*: **Phase II, randomized, placebo-controlled study of dovitinib in combination with fulvestrant in postmenopausal patients with HR(+), HER2(-) breast cancer that had progressed during or after prior endocrine therapy.** *Breast Cancer Res* 2017, **19**(1):18.
 52. Andre F, Bachelot T, Campone M, Dalenc F, Perez-Garcia JM, Hurvitz SA, Turner N, Rugo H, Smith JW, Deudon S *et al*: **Targeting FGFR with dovitinib (TKI258): preclinical and clinical data in breast cancer.** *Clin Cancer Res* 2013, **19**(13):3693-3702.
 53. Smyth EC, Turner NC, Pearson A, Peckitt C, Chau I, Watkins DJ, Starling N, Rao S, Gillbanks A, Kilgour E *et al*: **Phase II study of AZD4547 in FGFR amplified tumours: Gastroesophageal cancer (GC) cohort pharmacodynamic and biomarker results.** *Journal of Clinical Oncology* 2016, **34**(4_suppl):154-154.
 54. Babina IS, Turner NC: **Advances and challenges in targeting FGFR signalling in cancer.** *Nat Rev Cancer* 2017, **17**(5):318-332.
 55. Chae YK, Ranganath K, Hammerman PS, Vaklavas C, Mohindra N, Kalyan A, Matsangou M, Costa R, Carneiro B, Villaflor VM *et al*: **Inhibition of the fibroblast growth factor receptor (FGFR) pathway: the current landscape and barriers to clinical application.** *Oncotarget* 2017, **8**(9):16052-16074.
 56. Nogova L, Sequist LV, Perez Garcia JM, Andre F, Delord JP, Hidalgo M, Schellens JH, Cassier PA, Camidge DR, Schuler M *et al*: **Evaluation of BGJ398, a Fibroblast Growth Factor Receptor 1-3 Kinase Inhibitor, in Patients With Advanced Solid Tumors Harboring Genetic Alterations in Fibroblast Growth Factor Receptors: Results of a Global Phase I, Dose-Escalation and Dose-Expansion Study.** *Journal of clinical oncology : official journal of the American Society of Clinical Oncology* 2017, **35**(2):157-165.
 57. Matalkah F, Martin E, Zhao H, Agazie YM: **SHP2 acts both upstream and downstream of multiple receptor tyrosine kinases to promote basal-like and triple-negative breast cancer.** *Breast Cancer Res* 2016, **18**(1):2.

58. Chen YN, LaMarche MJ, Chan HM, Fekkes P, Garcia-Fortanet J, Acker MG, Antonakos B, Chen CH, Chen Z, Cooke VG *et al*: **Allosteric inhibition of SHP2 phosphatase inhibits cancers driven by receptor tyrosine kinases.** *Nature* 2016, **535**(7610):148-152.

Figure Legends

Figure 1. A genome-scale gain-of-function screen identified resistance genes to fulvestrant and GDC-0810. 17,255 human open reading frames (ORFs), corresponding to 10,135 distinct genes, were expressed in ER+ T47D breast cancer cells in the presence of fulvestrant or GDC-0810. 100 nM Fulvestrant, 1 μ M GDC-0810, or vehicle control (DMSO) was added following infection and selection. ORF representation was assessed by sequencing after 21 days of drug exposure. Genes that confer drug resistance will be enriched under drug selection, indicated by a positive log fold change (LFC) for ORF representation before and after DMSO/drug selection. **A**, The average Z score for LFC of each ORF was plotted for both the fulvestrant (X-axis) and GDC-0810 (Y-axis) arms. The average Z score was calculated from three replicates in each condition. The ORFs with a Z score > 3 in both drug arms are highlighted and labeled with gene ID. The shape of each data point represents the total number of ORFs for that gene in the library. **B**, Heatmap of top ORF hits with a Z score > 3 in fulvestrant or GDC-0810 arm. The Z score in the DMSO arm is also presented. ORF hits are grouped by their molecular function according to Uniprot annotation. Information on the complete list of ORFs can be found in Supplemental Table.1. **C**, Individual ORFs were overexpressed in T47D cells and validated to confer resistance to fulvestrant by drug response curves. *KRAS* G12D ORF was used for overexpression in T47D cells while other selected ORFs are wildtype. Cell viability was measured by CellTiter-Glo and all the data points were normalized to growth under DMSO condition. Results shown are \pm SD and representative of three independent experiments. **D**, Gene set enrichment analysis was performed for the gene list ranked by LFC in the fulvestrant arm. For genes with multiple ORFs, the ORF with

43

highest LFC was selected. 1000 permutations were performed for the analysis. NES, normalized enrichment score. The full list of nominated pathways is shown in Supplemental Table.2.

Figure 2. Identification of acquired FGFR and FGF alterations in metastatic biopsies from patients with resistant ER+ MBC. A, Evolutionary status of *ESR1*, *FGFR1*, *FGFR2*, *ERBB2*, and *FGF3* alterations is presented by comparing the pre-treatment and post-treatment mutational status for each patient (red = acquired, blue = lost, black = shared, grey = indeterminate). These 24 pairs of samples included 23 tumor biopsies and one cell-free DNA sample at the pre-treatment timepoint, and 22 tumor biopsies and two cell-free DNA samples at the post-treatment timepoint. The evolutionary inference of copy number changes was based on measuring differences in copy number amplitudes between pre-treatment and post-treatment samples, while accounting for differences in cancer cell fraction (“purity”) in the sample and correcting for differences in ploidy. The resultant purity-corrected values provide an estimate of “copy number above ploidy” (CNAP) (see Methods). The evolutionary inference and clonal dynamics of mutations was based on changes in the estimated fraction of tumor cells harboring each genomic alteration (the cancer cell fraction, CCF) as previously shown for acquired HER2 mutations [11]. Activating SNVs are denoted with a purple asterisk. Clinical and pathology tracks depict the site of biopsy for both matched samples, and the duration between the pre-treatment and post-treatment biopsies. The lines of endocrine therapies received between the early and late sample for a duration of at least 120 days are depicted with three tracks including SERD (Fulvestrant), SERM

(Tamoxifen), and any Aromatase Inhibitors (AI). **B**, Copy number alterations for *FGFR1*, *FGFR2* and *FGF3* in pre- and post-treatment tumor samples are shown with copy number above ploidy (CNAP) depicted to illustrate the magnitude of the acquired amplification in each case. To better measure segment-specific copy number, we subtracted the genome ploidy for each sample to compute CNAP. The purity and ploidy for tumor samples are shown in Supplemental Table.4. **C**, Clonal evolution analysis showing the overall clonal structure and acquisition for *FGFR2* mutations observed in two patients- *FGFR2* M538I (chr10:123258070C>T, GRCh37, also denoted as M537I, depending on the isoform) *FGFR2* N550K (chr10:123258034A>T, GRCh37, also denoted as N549K, depending on the isoform) In the pre-treatment biopsies, *FGFR2* M538I (*ID 0300348*) and *FGFR2* N550K (*ID 0300350*) were with cancer cell fraction (CCF) of 2% (single read) and 0% (unobserved), respectively, while being observed as clonal mutations in the post-treatment sample with a CCF of 1. The phylogenetic relationships among clones are reconstructed for each patient starting from the normal cell (white circle) connected to the ancestral cancer cells (grey trunk). The phylogenetic divergence to the pre-treatment clones (and subclones) is depicted with blue edges, and phylogenetic divergence to the metastatic clones (and subclones) is in red. Selected mutations in cancer genes are marked on the corresponding branches of the cancer phylogeny.

Figure 3. Clinical vignettes of patients who acquired FGFR/FGF alterations

following endocrine therapy. The clinical vignettes for selected patients with acquired alterations in *FGFR1*, *FGFR2*, and/or *FGF3* illustrate detailed information on age and

stage of disease at diagnosis, therapies patients received, duration of response to each therapy, and time of biopsies collected during the clinical course. For each biopsy, available information on biopsy type, tissue site, receptor status and selected genomic alterations detected by whole exome sequencing is shown. In each case, the asterisk indicates the time that metastatic disease was diagnosed. The complete clinicopathologic information for each patient is provided in Supplemental Table.7. IDC: invasive ductal carcinoma, IDLC: invasive ductal-lobular carcinoma; CNAP: copy number above ploidy; yo: years old; Bx: biopsy; PR: progesterone receptor; wt: wildtype.

Figure 4. Active FGFR signaling leads to resistance to SERDs and CDK4/6 inhibitors through activation of MAPK pathway. A, FGF ligands lead to resistance to fulvestrant, which was blocked by FGFR inhibitor PD173074. Recombinant FGF ligands were added into media every three days at the concentration of 100 ng/mL with or without 1 μ M PD173014. T47D cells were treated with heparin (1 μ g/mL) that facilitates the binding between FGF ligand and receptor, and sensitivity to 100 nM fulvestrant over six days was normalized to DMSO control. *** p-value < 0.001. Student t-test was performed for pair-wise comparisons. Results shown are \pm SD and representative of three independent experiments. **B,** FGFR1 or FGFR2 overexpression leads to resistance to fulvestrant, which was blocked by PD173074. GFP, FGFR1 or FGFR2 was overexpressed in T47D cells to establish stable T47D_GFP, T47D_FGFR1 and T47D_FGFR2 cells. The fulvestrant sensitivity of various cell lines were determined in the presence or absence of 10 ng/mL FGF2 and 1 μ M PD173074 over six days of drug treatment. Results shown are \pm SD and representative of three independent experiments.

C, FGFR1 and FGFR2 induced phosphorylation of ERK and AKT in the presence of FGF2, which was blocked by PD173074. Results shown are representative of two independent experiments. Cells were treated with indicated conditions for one hour before protein harvest. 10 ng/mL FGF2 and 1 μ M PD173074 were used. D, Trametinib abrogated the resistance to fulvestrant (top panel) or the combination of fulvestrant and palbociclib (bottom panel) conferred by FGFR1 or FGFR2. Cells were treated with different conditions as indicated: 10 ng/mL FGF2; 100 nM fulvestrant (Fulv); 1 μ M palbociclib (Palbo); 500 nM trametinib. CellTiter-Glo assay was performed to measure cell viability after six days for all dose response curves, data are \pm SD. Results shown are representative of three independent experiments. * p-value < 0.05, ** p-value < 0.01, *** p-value < 0.001, n.s. not significant. Student t-test was performed for pair-wise comparisons. E, Trametinib blocked ERK phosphorylation and reduced CCND1 and p-Rb levels. Cells were treated as indicated daily for two days before protein harvest and western blot: 10 ng/mL FGF2; 100 nM fulvestrant; 1 μ M palbociclib; 500 nM trametinib. Results shown are representative of two independent experiments.

Figure 5. FGFR2 M538I, N5550K and K660N were activating mutations and can be targeted by irreversible kinase inhibitors FIIN-2 and FIIN-3. A, Crystal structure of activated FGFR2 protein with mutations shown. FGFR2 is in complex with ATP analog (in yellow) and substrate peptide (PDB ID: 2PVF). FGFR2 N550K is part of the molecular brake at the kinase hinge region, which allows the receptor to adopt an active conformation more easily [35]. FGFR2 K660N is located in a conserved region in the tyrosine kinase domain and has been confirmed to increase kinase activity [34, 35]. B,

47

Stable cell lines overexpressing FGFR2 wildtype (WT), M538I, N550K, and K660N were treated with 10 ng/mL FGF2 and/or 1 μ M PD173014 for one hour before protein harvest. Results shown are representative of two independent experiments. **C**, Stable cell lines constitutively overexpressing GFP or FGFR2 constructs (as previously described) were examined for sensitivity to fulvestrant or combination of fulvestrant and palbociclib with or without the treatment of FGF2 and/or PD173074. * p-value < 0.05, ** p-value < 0.01, *** p-value < 0.001, calculated as compared to GFP group in all conditions. Student t-test was performed for pair-wise comparisons. Results shown are \pm SD and representative of three independent experiments. **D**, T47D cells overexpressing FGFR2 N550K cells were treated as indicated for three days and retreated for three hours before protein harvest and western blot. Results shown are representative of two independent experiments. **E**, All stable cells lines expressing GFP or FGFR2 constructs were treated with fulvestrant under the following conditions: control, 10 ng/mL FGF2, 10 ng/mL FGF2 with 1 μ M AZD4547, 10 ng/mL FGF2 with 1 μ M FIIN-2, or 10 ng/mL FGF2 with 100 nM FIIN-3. Drug response curves were determined by CellTiter-Glo. Results shown are \pm SD and representative of three independent experiments.

Figure 6. Transcriptional cell-state analysis of FGF/R activating perturbations reveals MAPK activation and ER-reprogramming, and FGFR-induced resistance phenotype was reversed by MEK and SHP2 inhibition. **A**, Linear Discriminant Analysis (LDA) projection of FGFR/FGF-activated cells and controls. Two-dimensional visualization of the transcriptional footprints driven by FGFR1, FGFR2, FGFR2 activating mutants, FGF3, and GFP (all shown as circles), as well as previously published

48

[11] transcriptional footprints of HER2 activating mutants, wild-type HER2, kinase-dead HER2 D845A, and ESR1 Y537S (all shown as triangles), all treated with DMSO.

“parental” refers to cells without ORF overexpression. **B**, Volcano plot representation of differentially expressed genes (DEGs) comparing the transcriptional footprints from cells expressing FGFR1, FGFR2, FGFR2 activating mutants, and FGF3, collectively vs.

controls, all under DMSO condition. The FGF/R-ACT transcriptional state was derived from significant DEGs. **C**, Selective volcano plots and GSEA plots indicate several

pathways which are activated in the FGF/R-ACT state, including RTK/Growth Factor Receptors signaling genes (624 genes), RAS/MAPK genes (701 genes), ER signaling driven by Growth Factors genes (95 genes), and MTOR pathway genes (953 genes). See

Supplemental Table.11 for gene sets, Supplemental Table.12 for a comprehensive list of gene sets and pathway associations. NES, normalized enrichment score; n.s. not

significant. **D**, RAS/MAPK signature was compared across various drug conditions for resistant FGFR/FGF cell lines. The signature strength for each sample is depicted in the Y-axis with a Z-score scaled across all 647 samples. Each box plot represents the

distribution of the signature strength among replicates of each experimental condition as indicated. Drug conditions include: “DMSO” (No Drug), “Fulv” (Fulvestrant), “Palbo”

(Palbociclib), “Fulv+Palbo” (Fulvestrant and Palbociclib), “FIIN-3”, “Fulv+FIIN-3”

(Fulvestrant and FIIN-3), “Palbo+FIIN-3” (Palbociclib and FIIN-3), “Fulv+Palbo+FIIN-

3” (Fulvestrant, Palbociclib and FIIN-3), “Fulv+Tram” (Fulvestrant and Trametinib),

“Fulv+Palbo+Tram” (Fulvestrant, Palbociclib and Trametinib. Concentration of drugs

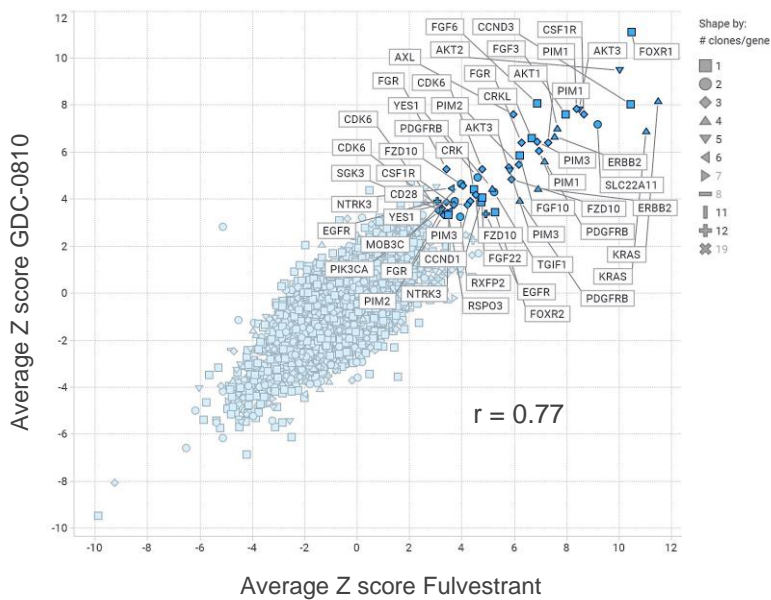
used: fulvestrant (100 nM), palbociclib (1 μ M), FIIN-3 (100 nM), trametinib (500 nM),

Construct perturbations include overexpression of GFP (Control), FGF3, FGFR1, and

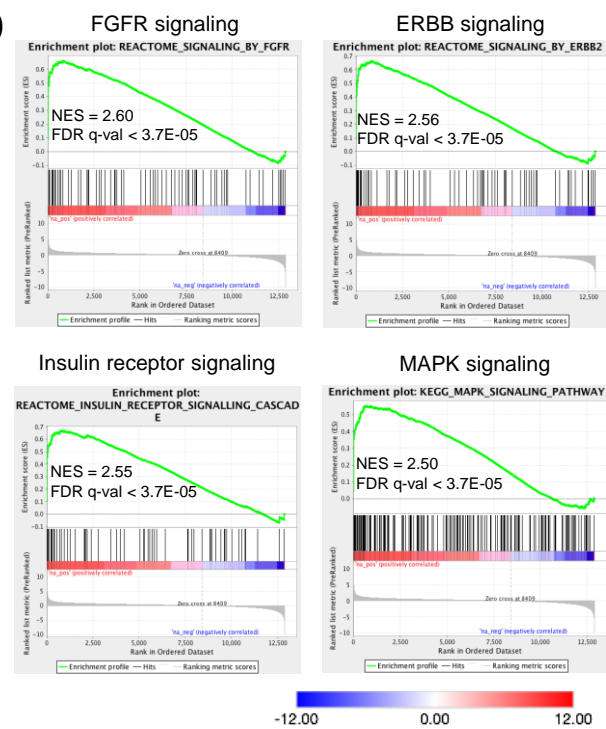
FGFR2 (WT, K660N, M538I and N550K). For cell lines overexpressing FGFR1/2, 10 ng/mL FGF2 was supplemented in the media. See Supplementary methods for details and Supplemental Table.11 for gene sets definitions. **E and F**, SHP099 as a single agent and in combination with trametinib rescued resistance to fulvestrant (E) and the combination of fulvestrant and palbociclib (F) conferred by FGFR1 or FGFR2 wildtype and mutant constructs. Concentration of drugs used: 10 ng/mL FGF2; 100 nM fulvestrant; 1 μ M palbociclib; 500 nM trametinib; 10 μ M SHP099. * p-value < 0.05, ** p-value < 0.01, *** p-value < 0.001. n.s. not significant. Student t-test was performed for pair-wise comparisons. Results shown are \pm SD and representative of three independent experiments.

Figure 1

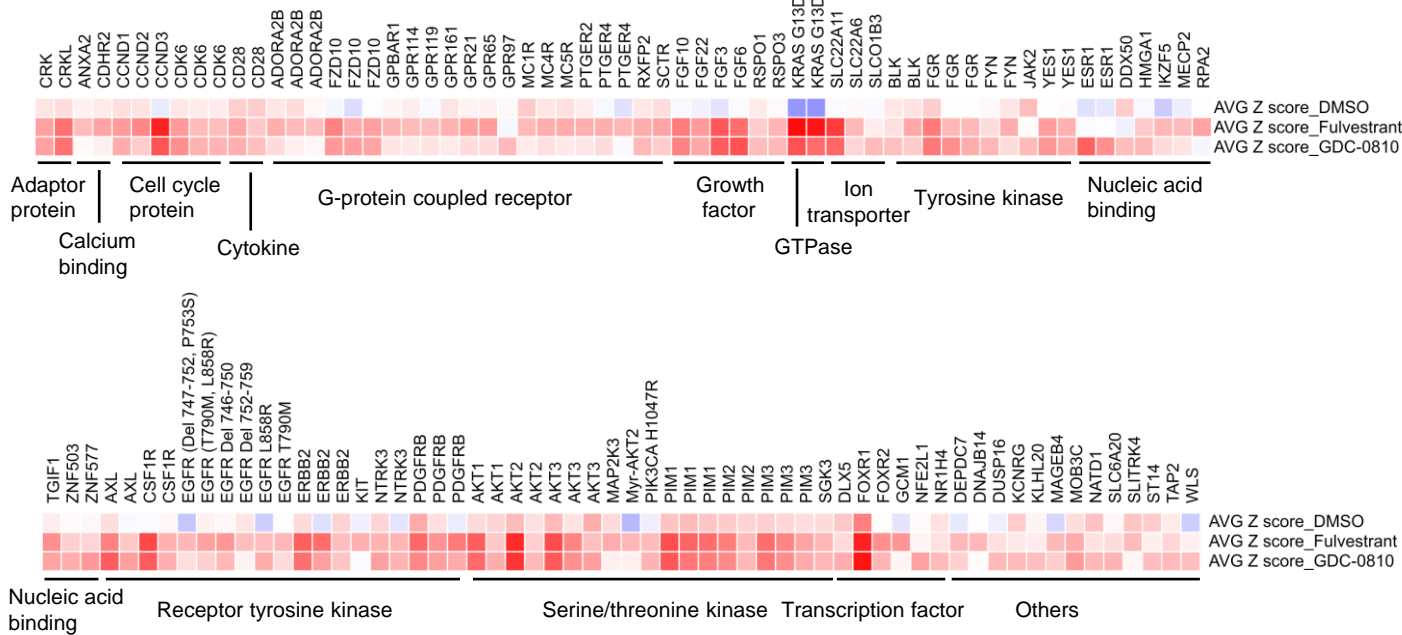
A



D



B



C

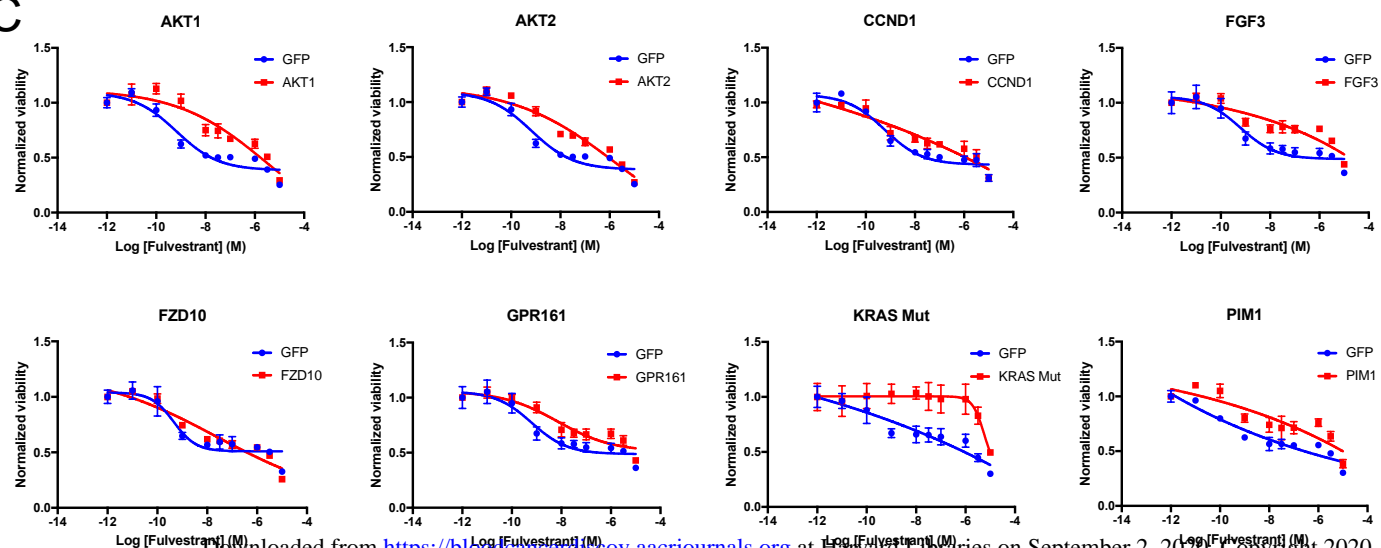


Figure 2

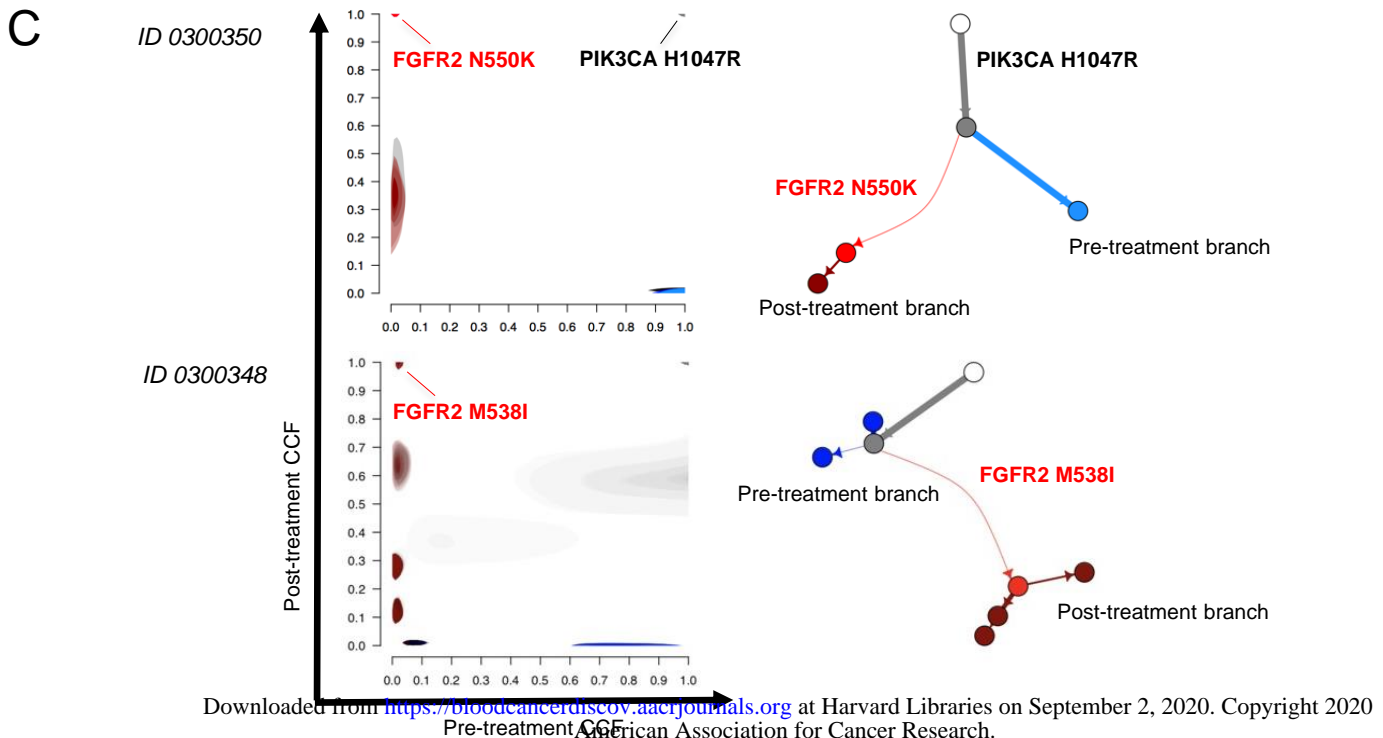
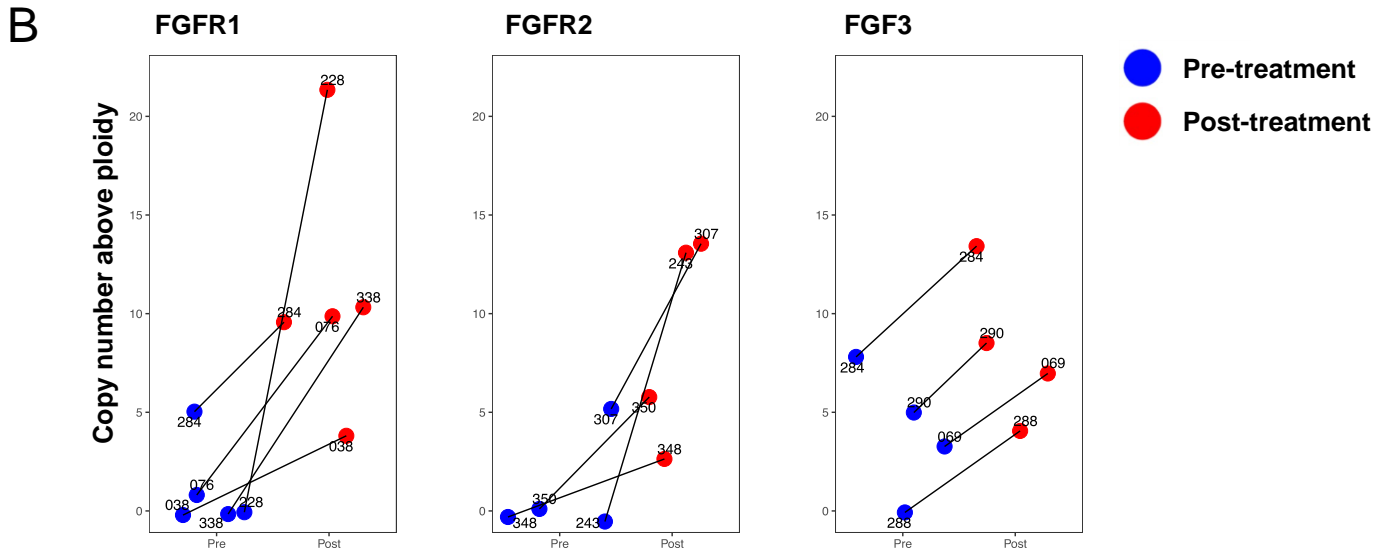
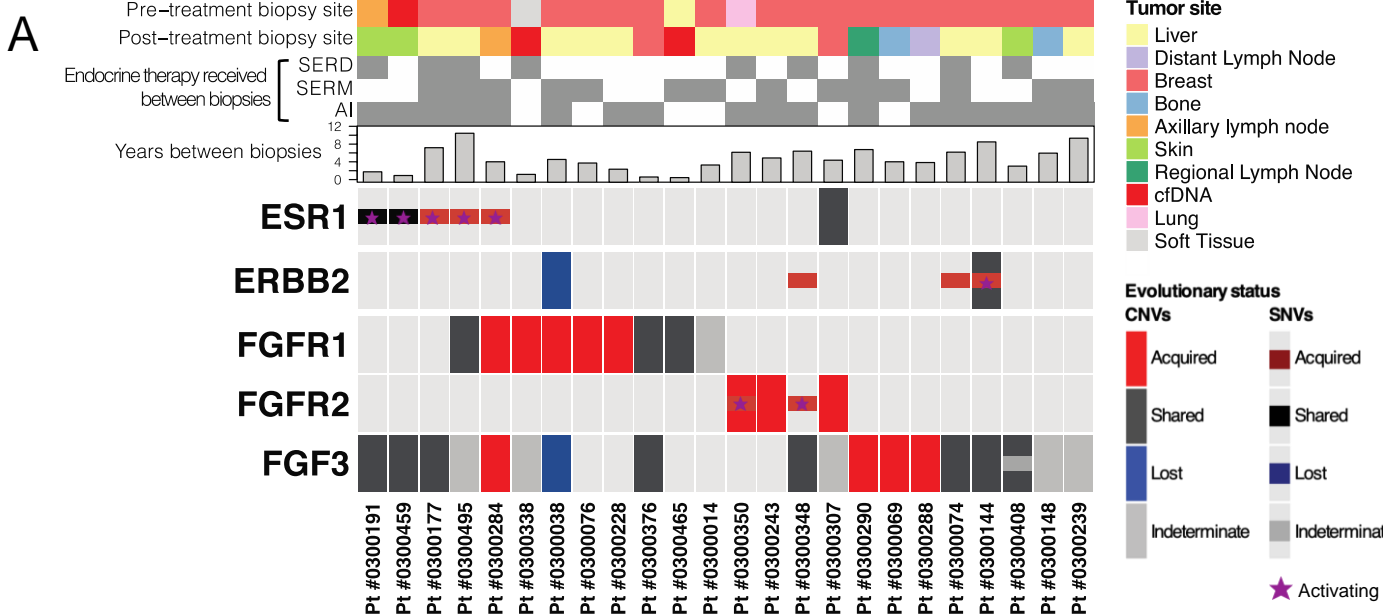


Figure 3

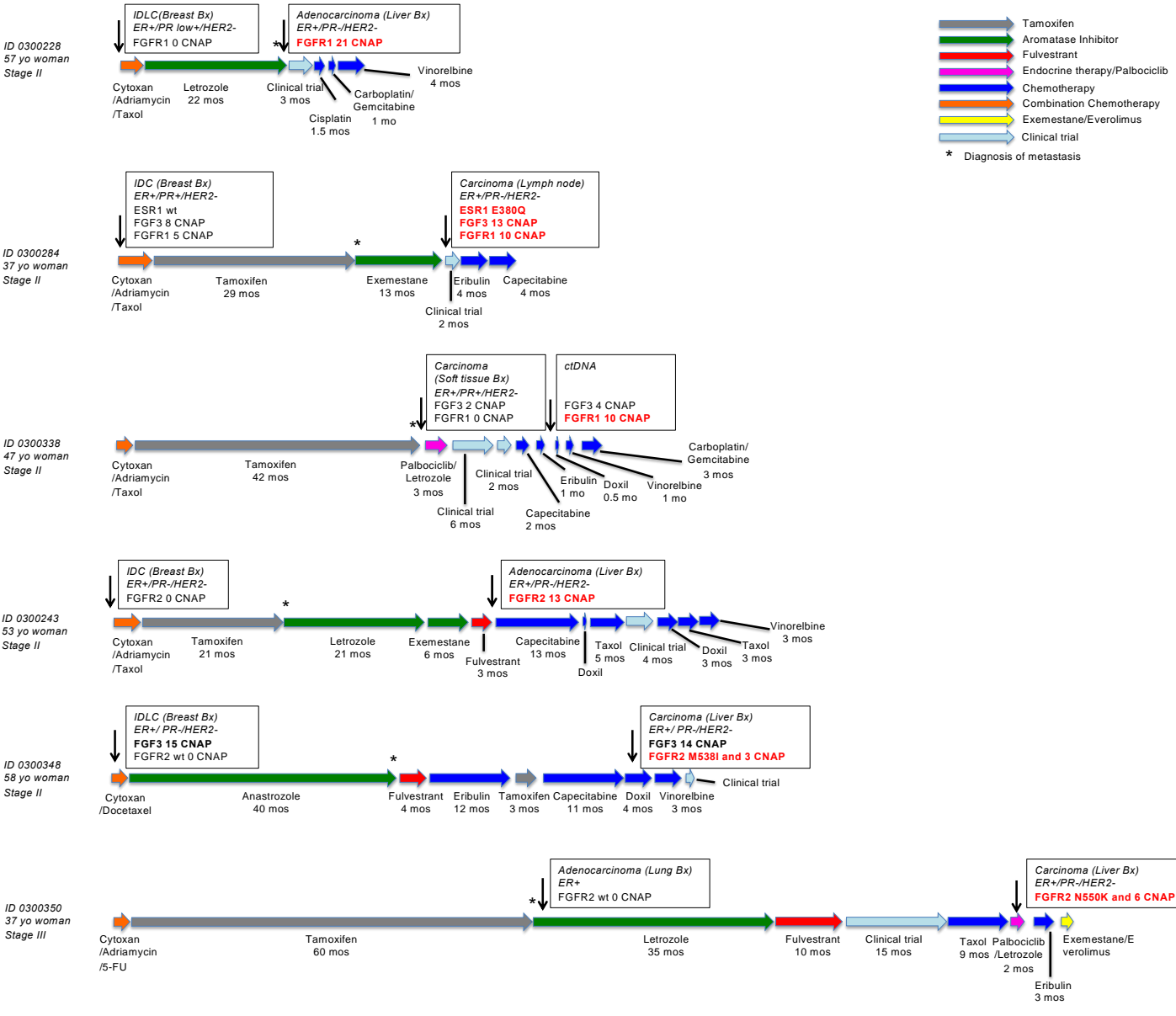
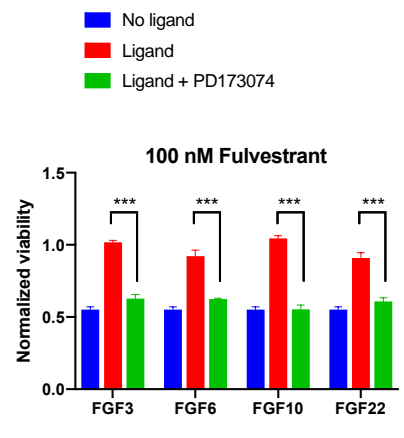
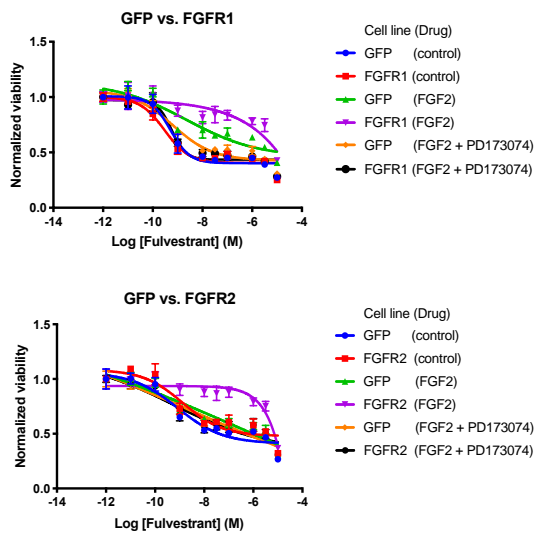


Figure 4

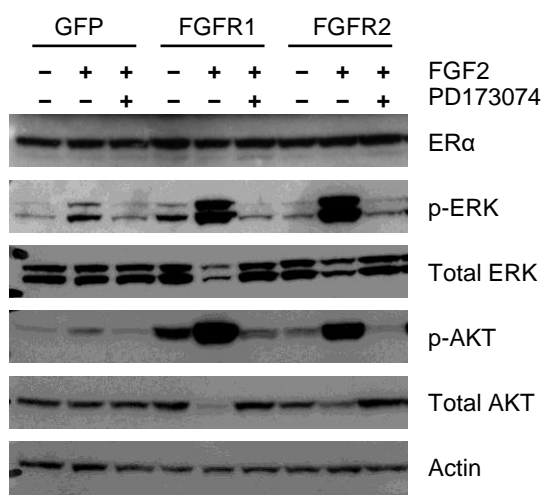
A



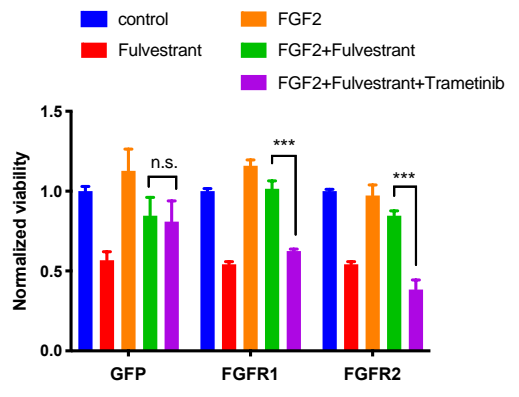
B



C



D



E

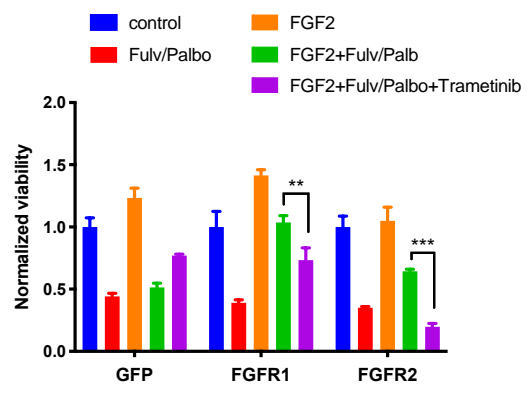
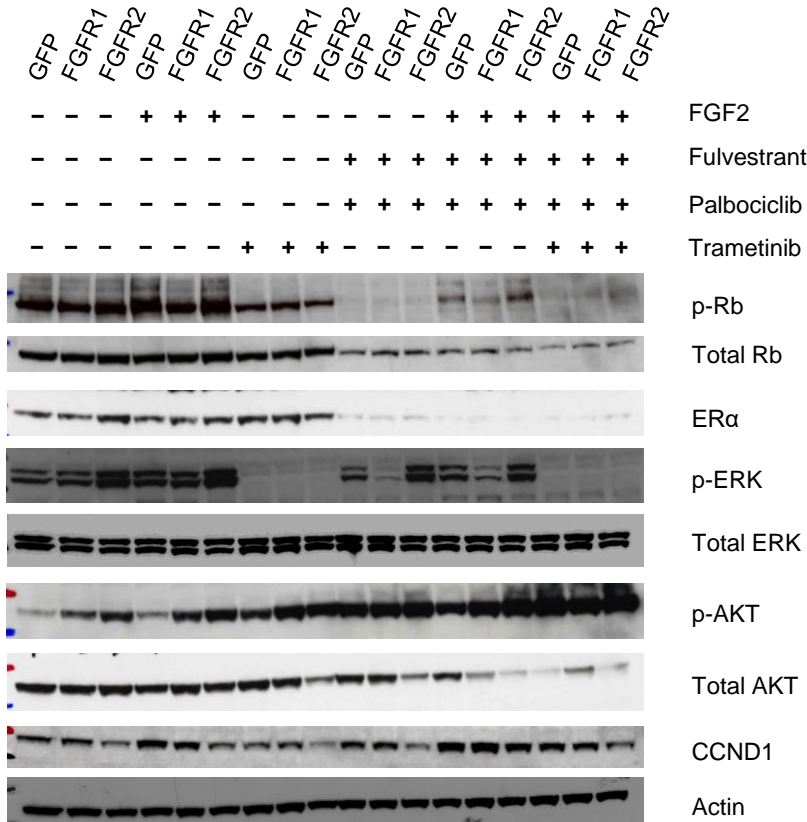


Figure 6

